Geochemical response of the mid-depth Northeast Atlantic Ocean to freshwater input during Heinrich events 1 to 4

Anya J. Crocker[1,2]*, Thomas B. Chalk[1,3], Ian Bailey[1,4], Megan R. Spencer[1], Marcus Gutjahr[1,5], Gavin L. Foster[1], Paul A. Wilson[1]

[1]National Oceanography Centre Southampton, University of Southampton, Waterfront Campus, Southampton SO14 3ZH, UK

[2]Department of Animal and Plant Science, University of Sheffield, Western Bank, Sheffield, S10 2TN, UK

[3]Now at: Department of Physical Oceanography, Woods Hole Oceanographic Institution, Woods Hole, Massachusetts, USA

[4]Now at: Camborne School of Mines & Environment and Sustainability Institute, College of Engineering, Mathematics & Physical Sciences, University of Exeter, Penryn Campus, Treliever Road, Penryn Cornwall, TR10 9FE, UK

[5]Now at: GEOMAR Helmholtz Centre for Ocean Research Kiel, Wischofstraβe 1 – 3, 24148 Kiel, Germany

*Corresponding author

Correspondence to: Anya J. Crocker, anya.crocker@noc.soton.ac.uk

Heinrich events are intervals of rapid iceberg-driven freshwater release to the high latitude North Atlantic Ocean that punctuate recent glacial intervals. Delivery of fresh water to the main North Atlantic sites of deep water formation during Heinrich events may result in major disruption to the Atlantic Meridional Overturning

Circulation, however, the simple concept of an AMOC shutdown in response to each freshwater input has recently been shown to be overly simplistic. Here we present a new multi-proxy dataset spanning the last 41,000 years that resolves four Heinrich events at a classic mid-depth North Atlantic drill site, employing four independent geochemical tracers of water mass properties: boron/calcium, carbon and oxygen isotopes in foraminiferal calcite and neodymium isotopes in multiple substrates. We also report rare earth element distributions to investigate the fidelity by which neodymium isotopes record changes in water mass distribution in the northeast North Atlantic. Our data reveal distinct geochemical signatures for each Heinrich event, suggesting that the sites of freshwater delivery and/or rates of input play at least as important a role as the stage of the glacial cycle in which the fresh water was released. At no time during the last 41 kyr was the mid-depth northeast North Atlantic dominantly ventilated by southern-sourced water. Instead, we document persistent ventilation by Glacial North Atlantic Intermediate Water (GNAIW), albeit with variable properties signifying changes in supply from multiple contributing northern sources.

Keywords: Heinrich events; North Atlantic palaeoceanography; Last glacial period; Neodymium isotopes; B/Ca; Carbon and oxygen isotopes; Ice-rafted debris; ODP Site 980.

1. Introduction

The climate of the last glacial period was punctuated by a number of pronounced events with near global impacts, known as Heinrich (or H-) events (e.g. Heinrich, 1988;

28 Hemming, 2004). During these events, transient catastrophic collapses of the North
29 American Laurentide Ice Sheet (LIS), centered over the Canadian Hudson Bay, produced
30 armadas of icebergs that travelled through the Hudson Straight into the North Atlantic
31 Ocean, eventually depositing large volumes of ice-rafted debris (IRD), including
32 distinctive detrital limestone clasts, in a belt across the North Atlantic (Ruddiman, 1977).
33 LIS surging, together with iceberg calving from other circum-North Atlantic and Arctic ice
34 sheets during H-events added large volumes of fresh (low density) water to the (sub)polar
35 oceans with important implications for northern- sourced deep water formation and the
36 Atlantic Meridional Over- turning Circulation (AMOC). The AMOC exerts a strong
37 control on regional and global climate on orbital to suborbital timescales, influencing
38 latitudinal heat budgets (e.g. Boyle and Keigwin, 1987; Broecker and Denton, 1989) and
39 partitioning of carbon between the atmosphere and deep ocean (e.g. Adkins, 2013; Sigman
40 and Boyle, 2000; Sigman et al., 2010). Understanding the response of AMOC to fresh
41 water addition is therefore crucial, particularly in light of recently accelerating mass loss
42 from the Greenland Ice Sheet and other circum-Atlantic ice masses (Gierz et al., 2015;
43 Vaughan et al., 2013).
44 Previously, it was suggested that fresh water inputs at high latitudes during H-
45 events caused a cessation of deepwater forma- tion in the North Atlantic, resulting in a
46 shoaling of the northern component water overturning cell by ~1 km (e.g. Alley et al.,
47 1999; Sarnthein et al., 1994; Swingedouw et al., 2009). Support for this concept of a near
48 complete shutdown of AMOC during H-events came from two main lines of evidence: (i)
49 a dramatic drop in circulation vigour (e.g. McCave et al., 1995a; McManus et al., 2004)
50 and (ii) water mass provenance reconstructions (including those based on $\delta^{13}C$, Cd/Ca and
51 ^{14}C) indicating an increased presence of nutrient-rich southern-source waters (SSW) below

~2e2.5 km depth in the North Atlantic Ocean (e.g. Keigwin et al., 1991; Robinson et al., 2005; Stern and Lisiecki, 2013; Vidal et al., 1997). More recently, however, both of these arguments have been questioned. $^{231}Pa/^{230}Th_{xs}$ records from sites across a wide range of water depths suggest that overturning persisted at shallower depths during H1 (Bradtmiller et al., 2014; Gherardi et al., 2009; Lippold et al., 2016), with values compatible with a near complete shutdown only identified in the SSW cell and during H-events close to glacial maxima (Bohm et al., 2015; Lippold et al., 2009; McManus et al., 2004). A further recent development is the documentation of a poorly ventilated water mass in the Nordic Seas during the last glacial period that overflowed the Greenland-Scotland Ridge (GSR) into the Atlantic basin during the deglaciation (Thornalley et al., 2015). This discovery means that the presence of nutrient-rich waters in the North Atlantic basin may no longer be simply attributed to the incursion of waters from the south. Indeed, excursions to low oxygen and sometimes also low carbon isotopic signatures of benthic foraminifera in the North Atlantic during H- events have been interpreted to suggest that there may also have been overflow of waters from the Nordic Seas at these times (e.g. Meland et al., 2008; Thornalley et al., 2010; Vidal et al., 1998). In addition, bulk sediment leachate ε_{Nd} values from the northeast North Atlantic (Crocket et al., 2011) are argued to support a persistent presence of overflow waters from the Nordic Seas in the North Atlantic throughout most, if not all, of the last glacial cycle, providing a northern source of nutrient-rich waters to the northeast Atlantic Ocean.

Detailed palaeoceanographic reconstructions show that the classic concept of a simple repeated response of AMOC to fresh- water addition during each H-event may be overly simplistic. Not all H-events show a clear perturbation in every oceanographic

reconstruction, and there is no consensus on which H-events involve the largest disruption of the ocean-atmosphere system. There is also little agreement about the factors that control the amplitude of AMOC response to freshwater input and considerable debate over the importance of H-event timing relative to the last glacial cycle (Bo€hm et al., 2015; Lynch-Stieglitz et al., 2014). New high-resolution data sets spanning multiple H-events are therefore needed to help us to gain a better understanding of the range of associated circulation changes in the Atlantic. Records from sites proximal to the GSR are particularly valuable because this region is especially sensitive to changes in northern deep water formation and therefore can help to better constrain variations in the influ- ence of Nordic Seas overflow waters (NSOW).

Bulk sediment leachate Nd isotope data from northeast Atlantic Ocean Drilling Program (ODP) Site 980 (55º29.1'N, 14º42.1'W; 2170 m water depth; location shown in Fig. 1) have been inter- preted to suggest that overflow waters crossing the Wyville-Thomson Ridge (WTR) from the Nordic Seas were supplied to the Feni Basin at intermediate depths for much of the past 41 kyr (Crocket et al., 2011), with either concentrated overflow waters without substantial entrainment of North Atlantic waters or SSW bathing the site during H-events 1e3. Yet, the potential for over- printing of water mass Nd isotope signatures in this region (Lacan and Jeandel, 2004a; Roberts and Piotrowski, 2015), concerns about the fidelity of bulk sediment leachate Nd isotope records (Elmore et al., 2011; Wilson et al., 2013) and the range of water masses influencing the intermediate-depth northeast North Atlantic (Lacan and Jeandel, 2005) are all sources of uncertainty demanding further careful assessment of the problem. Additional independent

proxies of water mass provenance are therefore required to help reconstruct past vertical water mass structure from the Feni Drift.

To address these gaps in our knowledge, we report the results of a new multi-proxy reconstruction of bottom water chemistry and inferred water mass distribution from ODP Site 980. First, we pre- sent neodymium isotope reconstructions from three phases (fish debris, planktonic foraminifera and bulk sediment leachates), together with rare earth element distributions to better understand the controls on neodymium association with foraminifera at Site 980. Then we combine our Nd isotope reconstructions with new, high resolution records of three further proxies for water mass chemistry (B/Ca, $\delta^{13}C$ and $\delta^{18}O$ in benthic foraminifera) at our study site to shed new light on the response of the AMOC in the northeast North Atlantic to freshwater addition during the H-events of the last glacial period.

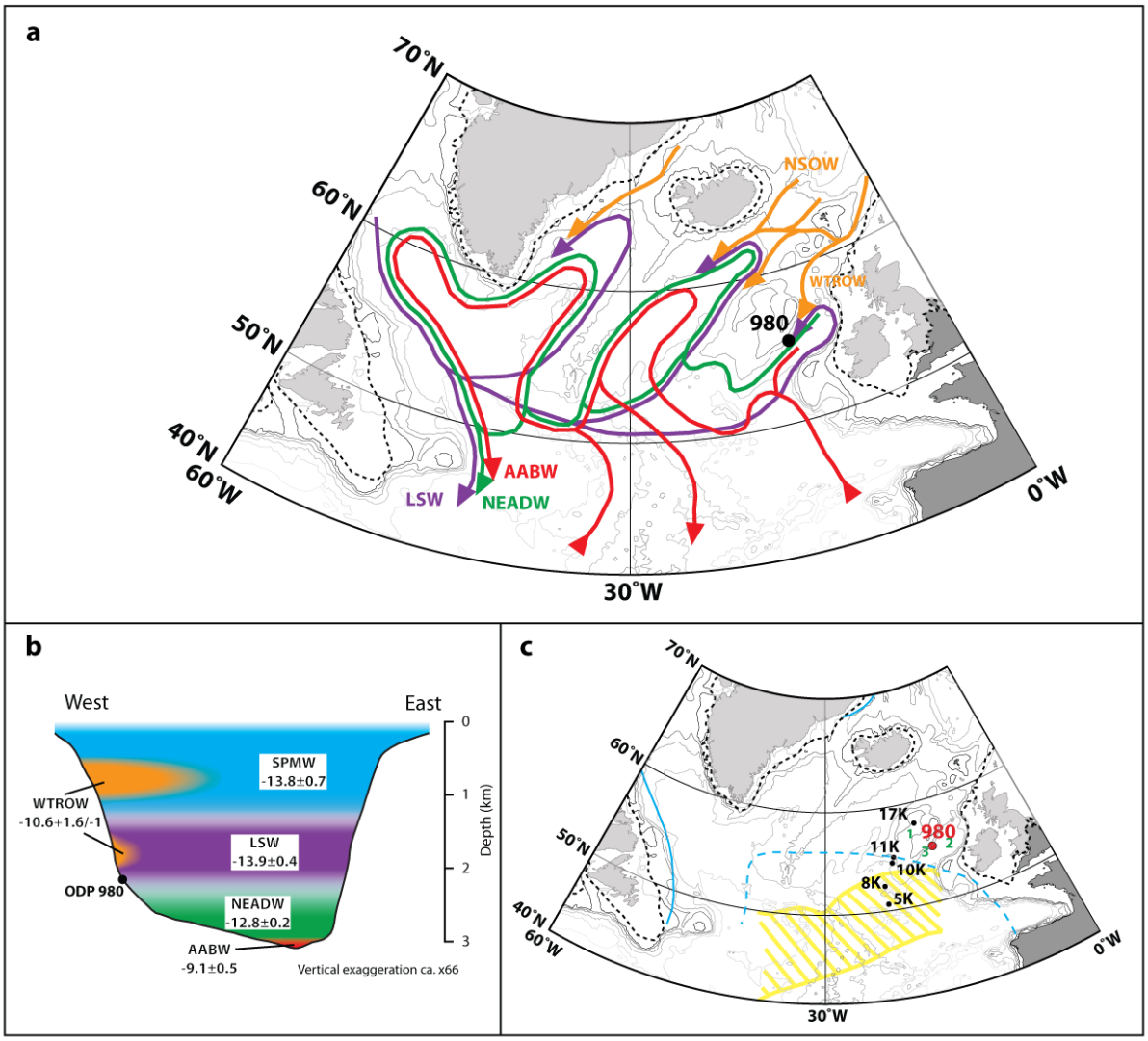

Fig. 1. (a) The North Atlantic region showing the location of the main study site (ODP Site 980, in black). Dotted lines mark the approximate maximum spatial extent of continental ice sheets during the last glacial maximum (Clark et al., 2012; Dyke et al., 2002; Funder and Hansen, 1996; Sejrup et al., 2005). Arrows represent modern major intermediate and deep current pathways with Nordic Sea overflows (NSOW, orange, also includes Wyville-Thomson Ridge overflow waters or WTROW), Labrador Sea Water (LSW, purple), Northeast Atlantic Deep Water (NEADW, light blue) and Antarctic Bottom Water (AABW, red), based upon McCartney (1992), Hansen and Østerhus (2000), New and Smythe-Wright (2001) and Lacan and Jeandel (2005). (b) Schematic cross-section of the major water masses in the modern Rockall Trough, based upon McGrath et al.

(2012) and Johnson et al. (2010). Colours as panel (a), with the addition of Subpolar Mode Water (SPMW, dark blue). Numbers give neodymium isotope signature of water masses today (Crocker, 2014; Crocket et al., 2011; Lacan and Jeandel, 2004c; Lacan and Jeandel, 2005; Lacan et al., 2012; Stichel et al., 2012). Note that the εNd value of AABW shown is the AABW endmember recorded in the Atlantic section of the Southern Ocean; this value is likely modified by mixing and boundary exchange as the water mass moves northwards (e.g. Lambelet et al., 2016). (c) North Atlantic region showing the location of the main study site (ODP Site 980, in red) and BOFS sites referred to in the text (black). Grey stripes indicate the main belt of ice-rafted debris deposition in the glacial north Atlantic during the Last Glacial Maximum (Ruddiman, 1977). Dark blue numbers: 1 e Rockall Plateau, 2 e Rockall Trough, 3 e Feni Drift. Last Glacial Maximum limit of perennial sea ice indicated by solid light blue line with dashed light blue line marking extreme limit of winter sea ice (de Vernal et al., 2005; Hillaire-Marcel and de Vernal, 2008).

2. Background

2.1 Site Location and Oceanography

ODP Site 980 is situated on the Feni sediment drift, and features high sedimentation rates (mean 20 cm kyr^{-1} across the studied interval, see details of age model in supplementary materials). Its position on the northern fringe of the main Atlantic belt of North American-sourced detrital carbonate deposition (Hemming, 2004) results in lithologically distinct and hence unambiguously identi- fiable Heinrich IRD layers. Site 980 is known for its benchmark archives of millennial-scale climate variability during the Quaternary (e.g. McManus et al., 1999; Oppo et al., 2003, 2006, Fig. 2). Existing records from this site cover an unusually long interval for suborbitally resolved records, extending back

144 approximately 500,000 years. Published data from Site 980 spanning the last glacial period
145 are, however, of insufficient resolution to resolve changes in ocean chemistry across H-
146 events clearly.

147 Today, Site 980 is bathed by a mixture of North East Atlantic Deep Water
148 (NEADW) and Labrador Sea Water (LSW), with only a minimal influence of Wyville
149 Thomson Ridge overflow waters (WTROW) from the Nordic Seas (Ellett and Martin,
150 1973; McGrath et al., 2012). During the last glacial period, Site 980 lay close to the
151 interpreted depth of the boundary between northern- and southern-sourced waters in the
152 North Atlantic (e.g. Boyle and Keigwin, 1987; Curry and Oppo, 2005; Oppo and Lehman,
153 1993), but is thought to have been bathed by Glacial North Atlantic In- termediate Water
154 (GNAIW) during background glacial conditions (Yu et al., 2008). If AMOC shutdown
155 occurred (as is classically suggested for last glacial H-events), model simulations suggest
156 that Site 980 would have been bathed instead by Glacial Antarctic Bottom Water
157 (GAABW) during these times (Flückiger et al., 2008; Singarayer and Valdes, 2010;
158 Swingedouw et al., 2009).
159

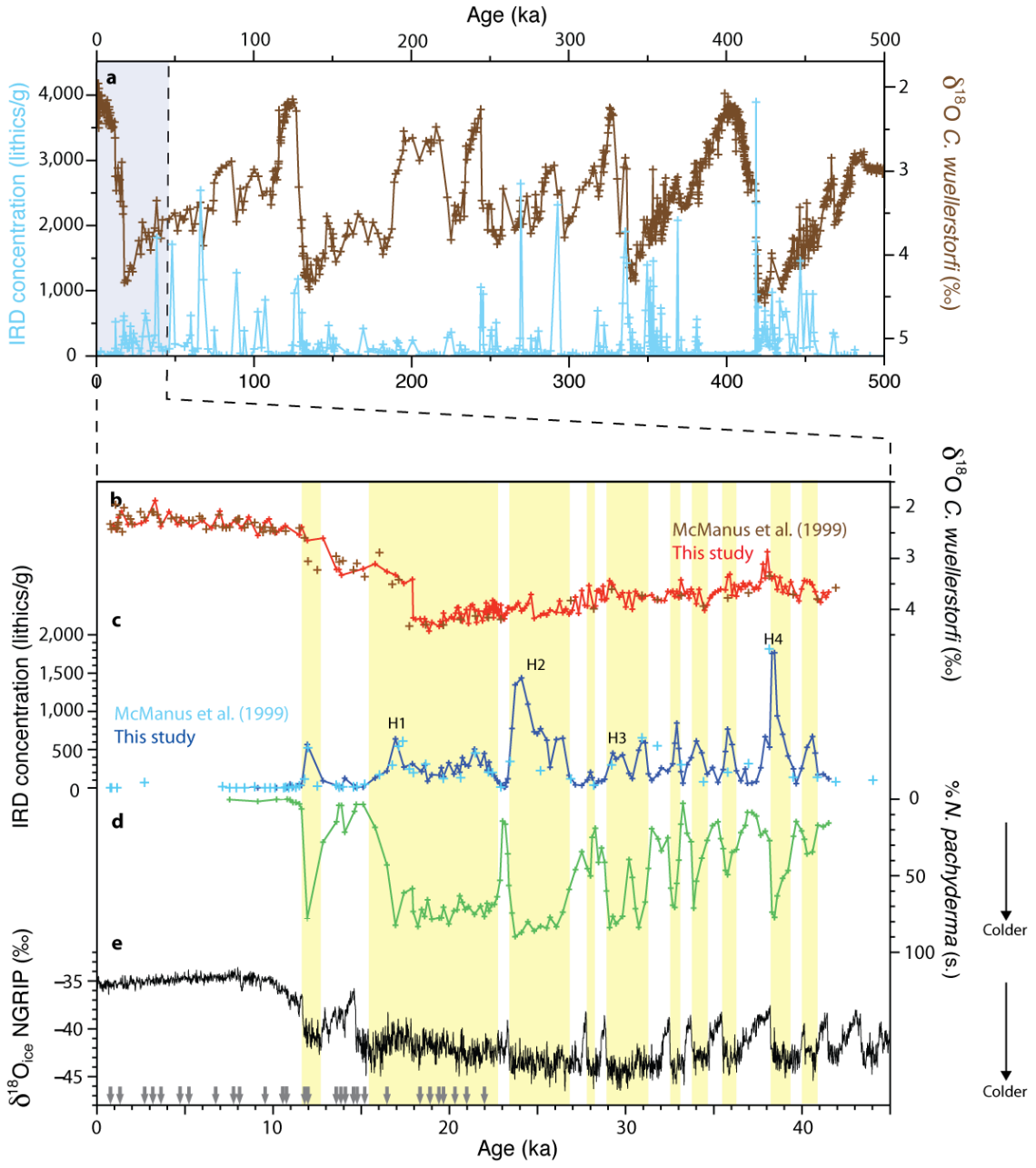

Fig. 2. Suborbital variability at ODP Site 980. (a) Data set of McManus et al. (1999), benthic foraminiferal oxygen isotopes in brown and IRD concentrations in pale blue. (b) New oxygen isotope record of benthic foraminiferal calcite (C. wuellerstorfi) in red (this study) with data of McManus et al. (1999) in brown (McManus data adjusted by 0.3‰ due to an inter-lab offset). (c) IRD concentrations, new data (this study) in dark blue (150e500 mm), data from McManus et al. (1999) in pale blue (grain size >150 mm). (d) Percentage of polar species N. pachyderma (s.) as a

proportion of the total number of planktonic foraminifera, with high values indicating cold sea surface temperatures (this study). (e) Oxygen isotope values of ice from NGRIP ice core, with less negative values indicating warmer temperatures (North Greenland Ice Core Project Members et al., 2004). NGRIP data plotted on the GICC05 age model (Andersen et al., 2006; Rasmussen et al., 2006; Svensson et al., 2008; Vinther et al., 2006). Grey arrows mark Site 980 recalibrated radiocarbon ages from Oppo et al. (2003) and Benway et al. (2010). Data in panels (b)–(d) are plotted on our new age model (see methods), with intervals of high ice rafting shaded in yellow.

2.2 Neodymium isotopes

Over the last few decades, neodymium isotopes have become an important tool for reconstructing the vertical structure of the water column and the provenance and circulation pathways of water masses. A major strength of the Nd isotope technique is that, unlike many commonly used proxies for water mass chemistry (e.g. $\delta^{13}C$), neodymium isotopes are not influenced by biological processes. The estimated residence time of Nd in the ocean (200e1000 years (Arsouze et al., 2009; Tachikawa et al., 1999, 2003)) is shorter than the modern oceanic mixing time of 1000e1600 years (e.g. Broecker and Peng, 1982; Garrison, 2011; Sarmiento and Gruber, 2004), giving rise to spatial variation in the isotopic signature of different water masses. Rocks exhibit a wide range of neodymium isotopic compositions, depending upon both their age and initial Sm/Nd ratios. These Nd isotope signatures are typically expressed in epsilon notation or εNd (representing the $^{143}Nd/^{144}Nd$ deviation of a sample relative to a chondrite uniform reservoir in parts per 10,000) with values ranging from $\varepsilon_{Nd} = -56$ for old granitic cratons to +12 for young mid-ocean ridge basalts (Jeandel et al., 2007; Lacan et al., 2012; Sarbas and Nohl, 2008, and references therein). Neodymium from this range of sources is transferred from the

191 continents to the ocean via both riverine and aeolian inputs, resulting in different water
192 masses acquiring distinct neodymium isotopic signatures (Goldstein et al., 1984; Grousset
193 et al., 1992; Mearns, 1988; Tachikawa et al., 1999). Addition and exchange of neodymium
194 at the sediment-bottom water interface along continental margins also modifies the
195 neodymium isotopic signature of bottom waters through the process of boundary exchange
196 (Lacan and Jeandel, 2004a; Rickli et al., 2014; Wilson et al., 2012).

197 Analysis of Fe-Mn oxyhydroxides within marine sediments extracted by a leaching
198 procedure (e.g. Gutjahr et al., 2007; Rutberg et al., 2000) allows the production of relatively
199 rapid and high resolution records of bottom water ε_{Nd}. This technique has now become
200 widely used (e.g. Bo€hm et al., 2015; Jonkers et al., 2015; Wei et al., 2015; Wilson et al.,
201 2015). A wide range of other phases have also been proposed to record and preserve bottom
202 water ε_{Nd}, including corals (e.g. Copard et al., 2010; van de Flierdt et al., 2006),
203 ferromanganese nodules and crusts (e.g. O'Nions et al., 1978; Piepgras et al., 1979), fish
204 debris (e.g. Lang et al., 2016; Martin and Haley, 2000; Staudigel et al., 1985) and
205 foraminifera both with and without authigenic Fe-Mn oxide coatings (e.g. Elmore et al.,
206 2011; Palmer and Elderfield, 1985).

207 The ε_{Nd} signatures recorded by different substrates do not al- ways agree with one
208 another (e.g. Elmore et al., 2011). For example, a pronounced difference between the
209 glacial and Holocene εNd values of uncleaned foraminifera is seen along a depth transect
210 of Biogeochemical Ocean Flux Study (BOFS) cores on and to the south of the Rockall
211 Plateau (Fig. 1), but this difference is muted or absent in co-registered bulk sediment
212 leachate ε_{Nd} (Piotrowski et al., 2012). The leaching of bulk sediment can give a neodymium
213 isotope signature influenced by reactive fine grained sediment components such as

214 volcanic ash (which has a radiogenic signa- ture) and detrital carbonate (which is
215 unradiogenic) (Elmore et al., 2011; Roberts et al., 2010), and thus bulk sediment leachates
216 may not accurately record bottom water chemistry at certain locations. The neodymium
217 isotope signature extracted by bulk sediment leaching is also highly sensitive to the
218 methodology used to sepa- rate the authigenic coating signal from the primary sediment
219 (Wilson et al., 2013).

220 The mostly constant value of ε_{Nd} 1⁄4 10 recorded by bulk sediment leachates from
221 Site 980 has been interpreted to demonstrate a continuous presence of WTROW in the
222 Rockall Trough for most, if not all, of the last 40 kyrs due to the similarity of this value to
223 the estimated signature of overflow waters (Crocket et al., 2011). In contrast, modern
224 oceanographic observations indicate only a minimal influence of WTROW at Site 980
225 today (Johnson et al., 2010; McGrath et al., 2012). Short-lived radiogenic Nd isotopic
226 excursions identified in the Site 980 record with ages estimated as approximately
227 concurrent to H-events 1–4 are inferred to record times of either increased influence of
228 SSW during AMOC shut- downs or a more concentrated presence of overflow waters
229 (Crocket et al., 2011). However, the limited resolution of the Site 980 bulk sediment
230 leachate ε_{Nd} dataset and the absence of direct identification of H-layers in the site
231 stratigraphy make these con- clusions tentative (see also supplementary material). In
232 addition, there are a number of other processes with the potential to alter bottom water εNd
233 (e.g. variable composition of NEADW or influence of LSW in the Rockall Trough,
234 modification of bottom water isotopic signature by interaction with lithogenic material).
235 The circulation history of the northeast Atlantic during the last glacial period therefore
236 requires further investigation.

A decoupling between ε_{Nd} values and other proxies used as water mass tracers ($\delta^{13}C$, B/Ca (Yu et al., 2008)) suggests that the glacial-interglacial variability in foraminiferal εNd on and to the south of the Rockall Plateau may not be a result of changing bottom water provenance (Roberts and Piotrowski, 2015). Instead, reactive IRD grains may modify water mass ε_{Nd} in this region as they sink through the water column, with large inputs of volcanic glass ($\varepsilon_{Nd} = +4.3 \pm 0.1$) to the Rockall Plateau and its southern flank appearing to modify bottom water towards more radiogenic values during the Last Glacial Maximum (Roberts and Piotrowski, 2015). Unradiogenic labelling of the water column by Hudson Bay-derived detrital limestone grains ($\varepsilon_{Nd} = -18.6 \pm 0.2$) may also have occurred during Heinrich events (Roberts and Piotrowski, 2015). These observations raise questions over the temporal and spatial extent of water mass ε_{Nd} relabelling.

To better understand the meaning of bulk sediment ε_{Nd} data from Site 980 and to investigate whether issues of water column relabelling by IRD identified on the Rockall Plateau and its southern margin are applicable to a wider area of the northeast Atlantic, we therefore need higher resolution ε_{Nd} records from multiple phases at Site 980 supplemented by a record of concentrations and lithologies of IRD. Furthermore, independent proxies of bottom water chemistry are also required to improve our understanding of water mass structure of the northeast Atlantic during the last 41,000 years at Site 980, therefore we also present co-registered benthic $\delta^{13}C$, $\delta^{18}O$, B/Ca records.

3. Materials and Methods

3.1 Stratigraphy

We sampled Holes 980B (0.05e4.12 m below seafloor (mbsf) at 8 cm resolution) and 980A (0.32–4.08 mbsf at 2 cm resolution). We sampled the same core sections as Crocket et al. (2011) to allow direct comparison with their data. Our Hole A samples are not part of the original primary shipboard splice (Shipboard Scientific Party, 1996), therefore, to assign composite depths (metres composite depth, mcd) to these samples, we correlated Hole A mbsf to the primary splice using shipboard-derived whole core volume- specific magnetic susceptibility data measured shipboard (see supplementary material) (Shipboard Scientific Party, 1996). Our study interval corresponds to 0.06e8.12 mcd.

3.2 IRD and % *N. pachyderma* (s.)

Sediment samples were sieved at 150–500 μm and then split until approximately 300 lithic grains remained, which were identified and counted using a binocular microscope, applying the categorizations of Hall et al. (2011). Pumice grains are assumed to have a volcanic ash origin, and so are not included in IRD counts. Reproducibility of IRD counts determined by repeat counts is ±1%. IRD fluxes were estimated following Peck et al. (2007), with bulk density values corrected for a systematic error in the ODP Leg 162 shipboard gamma-ray attenuation porosity evaluator (GRAPE) measurements (Jansen et al., 2000). Samples prepared for IRD counts were then split again until approximately 300 foraminifera remained. Counts were performed of the number of specimens of *Neogloboquadrina pachyderma* (sinistral) in these splits and the value expressed as a percentage of the total number of planktonic foraminifera. Reproducibility of % *N. pachyderma* (s.) values deter- mined by repeat counts is ±3%.

3.3 Stable isotopes

To generate benthic stable oxygen and carbon isotope reconstructions for our target interval, specimens of *Cibicides wuellerstorfi* (typically 2 – 4) were picked from the >212 μm size fraction (total carbonate mass 60 – 100 μg). Oxygen and carbon isotopic compositions of this carbonate were analysed using a Europa Geo 20-20 stable isotope ratio mass spectrometer at the University of Southampton. All sample values are expressed in delta notation, relative to the Vienna Peedee Belemnite standard (VPBD). External reproducibility is better than 0.053 ‰ for $\delta^{18}O$ and 0.027 ‰ for $\delta^{13}C$. Species-specific disequilibrium from seawater $\delta^{18}O$ values was corrected for by applying a correction factor of +0.64 ‰ (Shackleton and Opdyke, 1973). *C. wuellerstorfi* $\delta^{18}O$ values were adjusted for global sea level change ($\delta^{18}O_{ive}$) to allow us to understand temporal changes in regional water mass chemistry, following the method of Meland et al. (2008) and using the sea level record shown in Grant et al. (2012) with a maximum glacial-interglacial sea level change of 110 m.

3.4 Neodymium isotope ratios, rare earth elements and trace elements

3.4.1 Sample preparation

To generate neodymium isotope and rare earth element profiles from foraminifera, a large number (600–1600) of planktic foraminifera of mixed species were picked in the >212 μm size fraction from each sample. These were broken open then sonicated in ELGA water and methanol to remove clays, before being dissolved in 1.75 M HCl. Ferromanganese coatings were not removed from the foraminifera, as these are rich in pore water-derived Nd and have been shown to record a bottom water signature (Elmore et al., 2011; Roberts

306 et al., 2012).

307 Fish debris ε_{Nd} is considered to be a faithful recorder of the neodymium isotopic
308 composition of bottom waters (e.g. Grandjean et al., 1987; Martin and Haley, 2000;
309 Staudigel et al., 1985; Stille, 1992; Stille and Fischer, 1990). To provide an additional
310 check on the fidelity of our new foraminiferal ε_{Nd} record, we therefore picked 1e15 pieces
311 of fish debris from the >125 mm size fraction of a subset of samples (n = 8). Adhering
312 clays were removed by sonication in methanol and ELGA water. All samples were
313 oxidatively cleaned based upon the methods of Boyle and Keigwin (1985), although a
314 reductive cleaning step was not necessary (Martin and Haley, 2000). An aliquot of 10 ml
315 was extracted from each of the dis- solved foraminifera and fish debris samples for rare
316 earth element (REE) and other trace element analysis, with the remainder of the sample
317 used for neodymium isotope analysis.

318

319 3.4.2 Rare and trace elements

320 The mechanism by which Nd becomes associated with foraminifera strongly influences
321 whether the isotopic signature preserved is representative of the bottom water signature
322 (Roberts et al., 2012; Tachikawa et al., 2014). The extent of remobilization of Nd in
323 sediment pore waters is of particular interest, and can be investigated using REE
324 concentrations and distributions (Roberts et al., 2012). Subtle differences in the behaviour
325 of the various REEs result from a decrease in atomic radius as mass increases, leading to
326 differences in their speciation in seawater (Elderfield and Greaves, 1982; Goldberg et al.,
327 1963). The behaviour of cerium is also distinct from the other elements because it can be
328 oxidized from a soluble (3+) to an insoluble (4+) state (de Baar et al., 1985; Elderfield et

329 al., 1988). This distinction can be expressed by the cerium anomaly (Ce/Ce*), which is the
330 difference in the shale-normalised abundance of cerium compared to the expected value
331 calculated from the nearby light rare earth (LREE) elements ($Ce/Ce^*=3Ce_n/(2La_n+Nd_n)$,
332 where $_n$ indicates concentrations relative to the Post-Archean Australian Shale, PAAS
333 (McLennan, 1989; Taylor and McLennan, 1985)). Negative cerium anomalies (values <1)
334 indicating a depletion of cerium relative to the other REEs (de Baar et al., 1988).
335 Rare earth element samples were diluted with 3% HNO_3 spiked with In, Re and Be.
336 Calcium and strontium concentrations were measured with a Quadrupole ICP-MS: Thermo
337 X-Series 2 at the University of Southampton. The remaining sample solutions were
338 analysed for REE and trace element concentrations using the High Resolution ICP-MS:
339 Thermo ELEMENT 2XR at the University of Southampton. All samples were corrected
340 for matrix effects and instrument drift using the In, Re and Be standard incorporated into
341 each sample. A blank correction was then applied and rare earth element standards used to
342 correct samples for oxide formation. External reproducibility is estimated as 4–5 %, with
343 internal reproducibility much less than this for the majority of samples. Rare earth element
344 concentrations of the samples (REE_{sample}) were expressed relative to the REE signature of
345 the PAAS (REE_{PAAS}) (McLennan, 1989; Taylor and McLennan, 1985).
346
347 3.4.3 Neodymium isotope ratios
348 Neodymium was purified from the dissolved samples for isotope analysis using standard
349 procedure column chemistry, based upon the methods of Cohen et al. (1988). Cation
350 columns were used to strip iron and titanium from the samples. The remaining material
351 was then run through LN Spec^{TM} columns to isolate neodymium (Pin and Zalduegui, 1997).

352 Samples were analysed by the Multi-collector ICP-MS: Thermo NEPTUNE at
353 Southampton. Instrumental mass bias ratios were corrected using the procedure of Vance
354 and Thirlwall (2002), adjusting to a $^{146}Nd/^{144}Nd$ of 0.7219 and using cerium-doped
355 standards to correct for interference of ^{142}Ce on ^{142}Nd. All values were normalised to the
356 JNdi-1 Standard ($^{143}Nd/^{144}Nd = 0.512115\pm7$) (Tanaka et al., 2000), and isotopic signatures
357 are expressed in epsilon notation, using a chondritic uniform reservoir value of 0.512638
358 (Jacobsen and Wasserburg, 1980). Replicate measurements of the JNdi-1 standard across
359 the three runs gave an external reproducibility 2 s.d. = 0.2 ε_{Nd} units for replicate analyses
360 of Nd standard solutions (n = 25). Error bars plotted show either this external
361 reproducibility or the sample internal reproducibility, whichever is larger. We compared
362 our Nd data to co-measured concentrations of lithophilic elements (e.g. Al, Ti, Zr, Pb) and
363 volcanic grains, and find no evidence to suggest a strong control of volcanic ash, clay
364 contamination or other terrestrial material on foraminiferal ε_{Nd} values at Site 980 (see
365 supplementary information).
366
367 3.5 Boron/calcium ratios
368 Between 8 and 12 *C. wuellerstorfi* tests (212 – 500 μm) were cleaned for trace metal
369 analysis following Barker et al. (2003). Foraminiferal tests were cracked and ultrasonicated
370 in Milli-Q 18.2 MΩcm water to remove clay materials. Samples are then oxidatively
371 cleaned in a 1% hydrogen peroxide solution before a weak acid leach is applied to remove
372 adsorbed cations. Finally, samples are dissolved in ~ 0.075M nitric acid. The above steps
373 were all undertaken in a specialised boron free clean laboratory at the University of
374 Southampton. Element ratios were analysed on a ThermoFisher Scientific Element 2XR-

375 ICPMS at Southampton, using the protocol described by Rae et al. (2011) employing
376 matrix matched in house standards and a variety of consistency standards to ensure
377 reproducibility. Samples were screened for clay contamination using Al/Ca and other
378 contaminant ratios (e.g. Ba/Ca, Fe/Ca), with samples Al/Ca > 100 μmol/mol excluded from
379 this study (n = 2). No anomalous values of other elements were identified. Near complete
380 clay removal is assumed for the remaining samples. Long-term reproducibility for B/Ca
381 for the duration of this study is within 4 % at 2 s.d. (~8 μmol/mol). Carbonate ion
382 concentrations were calculated using a sensitivity of $\Delta[CO_3^{2-}]$ on B/Ca of 1.14 ± 0.048 for
383 *C. wuellerstorfi* (Yu and Elderfield, 2007), and a $[CO_3^{2-}]_{sat}$ calculated from local pressure,
384 temperature and salinity.
385
386 3.6 Age model generation
387 A new age model was developed for Site 980 by combining previously published
388 radiocarbon ages (Benway et al., 2010; Oppo et al., 2003) with a new record of the
389 abundance of planktonic foraminifera *N. pachyderma* (s.) correlated to Greenland proxy
390 re-cords (Fig. 2 and supplementary information). An average sedimentation rate of ~0.2
391 mm/yr means that samples with 2 cm spacing give an age resolution of approximately 100
392 years.
393 Radiocarbon ages were updated using the Marine13 calibration curve (Reimer et
394 al., 2013) in conjunction with Calib 7.1 software (Stuiver and Reimer, 1993; Stuiver et al.,
395 2005). A constant reservoir age of 400 ± 100 years was assumed, with the exception of the
396 Younger Dryas (800 ± 300 years) and H1 (1600 ± 1000) (e.g. Bard, 1988; Bard et al., 1994;
397 Bondevik et al., 2006; Stanford et al., 2011; Stern and Lisiecki, 2013; Waelbroeck et al.,

2001). Additional age constraints were provided by correlating the Site 980% N. pachyderma (s.) record (a proxy for upper ocean temperature when sea surface temperatures are between 4˚C and 10˚C (Darling et al., 2006)) to North Greenland Ice Core Project (NGRIP) $\delta^{18}O_{ice}$ (a proxy for atmospheric temperatures) (North Greenland Ice Core Project Members et al., 2004) on the GICC05 age model (Andersen et al., 2006; Rasmussen et al., 2006; Svensson et al., 2008; Vinther et al., 2006). Visual correlation was carried out using the Analyseries software (Paillard et al., 1996), and is based on the assumption that temperature changes in the upper North Atlantic Ocean were synchronous with Greenland air temperatures. Distinctive peaks in detrital carbonate fluxes were used to confirm the position of H4, H2 and H1.

4. Results and Discussion

4.1 Assessing the validity of neodymium isotopes as a water mass tracer at ODP Site 980

4.1.1 Exploring inter-substrate differences in neodymium isotope signatures

New records of REE distributions and Nd isotope signatures of mixed planktonic foraminifera and fish debris from Site 980 are shown together with IRD concentrations in Fig. 3. Throughout our study interval, there is close agreement between new data from fish debris and planktonic foraminifera ε_{Nd} data. Glacial ε_{Nd} values recorded by fish and foraminifera (-9 to -10) are more radiogenic than Holocene values (~-11.5), with suborbital unradiogenic ex- cursions from baseline values during H4 (~38 ka) and the early Holocene

(~5–8 ka), and a strong radiogenic excursion across H2 (~23–26 ka) (Fig. 3a). Previously published sediment leachate ε_{Nd} data from Site 980 (Crocket et al., 2011) generally show a systematic offset towards more radiogenic values than our new foraminifera and fish debris values by 1–2 ε_{Nd} units over the last ~11.5 ka (Fig. 3a). This systematic offset is not present in the samples of peak glacial age, where agreement between the two substrates is often much closer, although there are some sporadic disagreements between the two records.

Modern oceanographic observations show that the mid-depth western Rockall Trough is predominantly bathed by NEADW (ε_{Nd} -12.8 ± 0.2) and LSW (-13.9 ± 0.4), with a small influence of overflow waters from the Nordic Seas (-8.2 ± 0.6) (Ellett and Martin, 1973; Johnson et al., 2010; Lacan and Jeandel, 2005; McGrath et al., 2012; Olsen and Ninnemann, 2010). This suggests that the youngest foraminiferal ε_{Nd} values at Site 980 (-11.7 ± 0.3) capture bottom water chemistry more accurately than bulk sediment leachate ε_{Nd} (-10.2 ± 0.3). A stronger overflow signature than indicated by modern observations (Johnson et al., 2010) or local modification of bottom waters towards more radiogenic values is required if the youngest leachate ε_{Nd} signatures at our study site accurately represent recent bottom water chemistry. Alternative explanations include analytical issues offsetting the bulk sediment leachates to more radiogenic values than the fish debris and foraminifera, and the influence of an additional radiogenic phase shifting bulk sediment leachates towards more radiogenic values in the Holocene.

Bulk sediment leachates can provide a relatively rapid way to reconstruct seawater chemistry, but a number of studies have highlighted the sensitivity of the technique to the precise method used. Wilson et al. (2013) and Blaser et al. (2016) have recently shown that carbonates play an important role as a buffer when extracting the ferromanganese coatings

444 from sediments, preventing the acid-induced mobilization of Fe oxides and volcanigenic
445 material (which has the potential to shift the measured ε_{Nd} towards more radiogenic values).
446 Crocket et al. (2011) followed the earlier procedure of Gutjahr et al. (2007) which included
447 a prior decarbonation step. Leaching time, sample size and pH have also been shown to
448 influence the bulk sediment leachate ε_{Nd} signature (Blaser et al., 2016; Wilson et al.,
449 2013).

450 Radiogenic offsets of bulk sediment leachate ε_{Nd} values from foraminiferal Nd
451 signatures have also been documented in core top samples at other sites in the North
452 Atlantic and attributed to the influence of volcanic ash that is easily leached during the
453 extraction process (Elmore et al., 2011). There is no evidence, however, for increased or
454 sustained volcanic activity throughout the Holocene that would increase the accumulation
455 rate of ash in the sediment at Site 980 (see supplementary information). Instead, North
456 Atlantic ash deposition is much more frequent during the last deglaciation (e.g. Abbott and
457 Davies, 2012; Davies et al., 2012; Lowe et al., 2008), when very good agreement exists
458 between foraminiferal and bulk sediment leachate ε_{Nd} at Site 980. Airborne volcanic ash
459 therefore cannot easily be invoked to explain the observed offset between substrates during
460 the Holocene.

461 Variable transport of silt-sized titanomagnetite grains from the GSR by bottom
462 currents has been documented at a number of sediment drift sites that lie in the path of
463 overflow waters. Higher accumulation of titanomagnetite is documented associated with
464 higher current velocities under interstadial conditions compared to stadials, with grains
465 likely originating from the young basaltic (and radiogenic) rocks of the Nordic Basaltic
466 Province (Ballini et al., 2006; Kissel, 2005; Kissel et al., 1999). Bottom currents were

467 generally much stronger in the Holocene than the glacial in the North Atlantic (Innocent et
468 al., 1997; Manighetti and McCave, 1995; McCave et al., 1995a; McIntyre and Howe, 2009;
469 McManus et al., 2004; Thornalley et al., 2013), therefore, increased accumulation of
470 leachable fine material at the Feni Drift during the Holocene represents a possible
471 alternative explanation for the more radiogenic signature recorded by Site 980 sediment
472 leachates. There is a possibility that certain other drift deposits in the region may be
473 susceptible to a similar process because the spatial distribution of sites showing
474 unreasonably radiogenic core top sediment leachate ε_{Nd} values (as identified by Elmore et
475 al. (2011)) agrees well with the major pathways of modern Nordic Overflow waters (e.g.
476 Hansen and Østerhus, 2000), and bulk sediment leachate ε_{Nd} records showing the largest
477 radiogenic offset compared to other substrates during the Holocene have been reported at
478 some other sites in the North Atlantic (Piotrowski et al., 2012; Roberts et al., 2010).
479 We conclude that the influence of bottom current transported, silt-sized radiogenic
480 particles on sediment leachate εNd is the most likely explanation for the offset between the
481 Nd isotope substrates during the Holocene at our study site, with the leachate method also
482 contributing to the variable offsets throughout the record. This implies that published bulk
483 sediment leachate values are not an accurate record of bottom water chemistry at Site 980,
484 at least in the uppermost sedimentary column (above 2.9 mcd). As a consequence, we only
485 consider the Nd isotopic signatures of foraminifera and fish debris as potential tracers of
486 water mass provenance at Site 980.
487
488

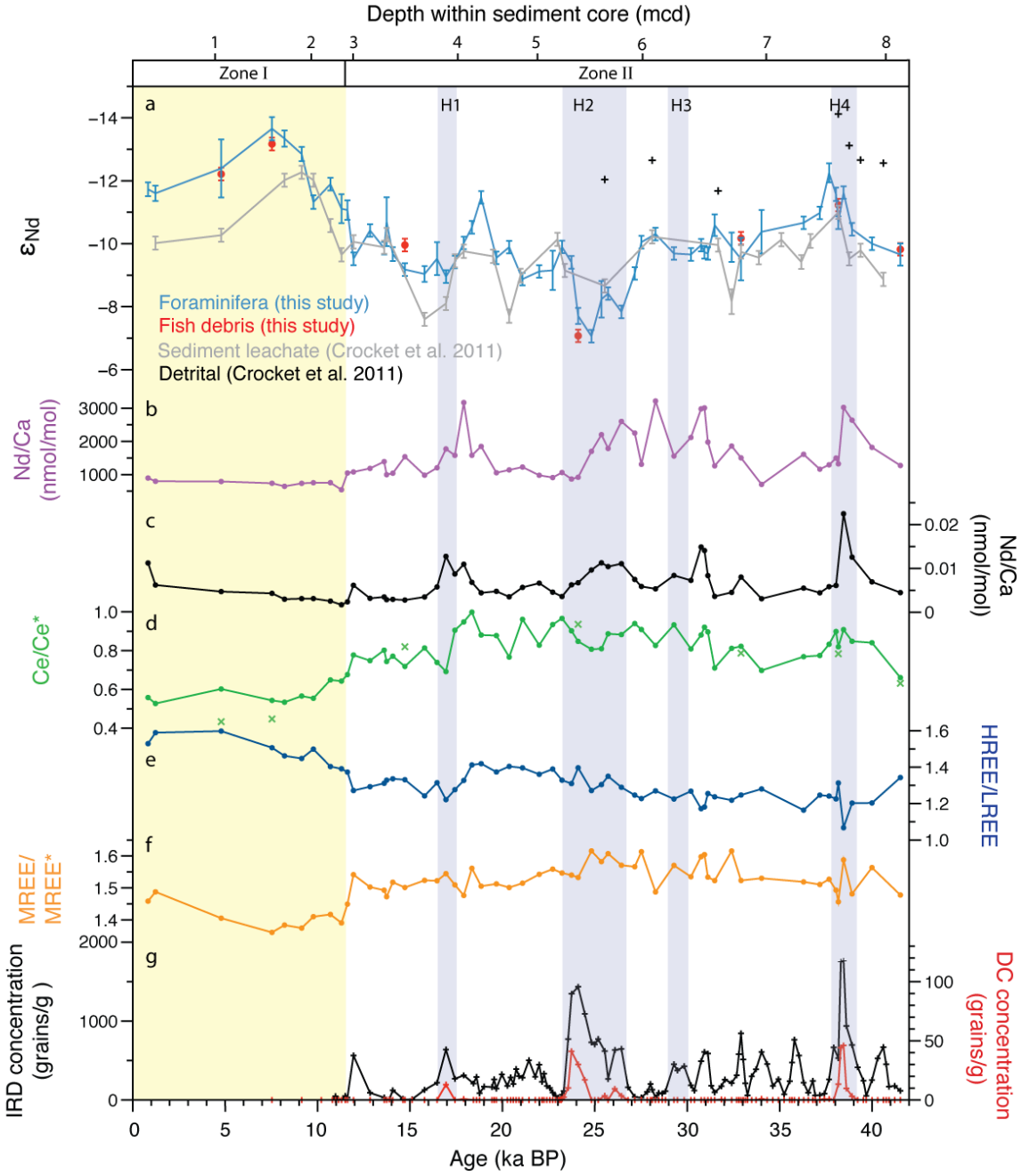

489

490 Fig. 3: ODP Site 980 neodymium isotope and rare earth element chemistry. (a) Neodymium isotope
491 composition (and 2σ error) of mixed planktonic foraminifera (blue), fish debris (red), sediment
492 leachates (grey, (Crocket et al., 2011)) and the detrital fraction (black, (Crocket et al., 2011)). (b)
493 and (c) Nd/Ca and Nd/Mn ratios of mixed planktonic foraminifera. (d), (e) and (f) Ratios of mixed
494 planktonic foraminifera PAAS-normalised REEs (X_n) with (d) Ce/Ce* = $3Ce_n/(2La_n+Nd_n)$, (e)

HREE/LREE = $(Er_n+Yb_n+Lu_n)/(La_n+Pr_n+Nd_n)$, (f) MREE/MREE* = $Gd_n+Tb_n+Dy_n/0.5(La_n+Pr_n+Nd_n+Er_n+Yb_n+Lu_n)$. Fish Ce/Ce* ratios are shown by crosses in panel (d). (g) Fluxes of ice-rafted debris (black) and detrital carbonate (red) grains from the 150 – 500 μm size fraction. Purple shading marks the timing of Heinrich-layer deposition (identified from the IRD and detrital carbonate records). Yellow shading highlights the upper section of the core with an offset in the Nd isotope ratios between the planktonic foraminifera and fish debris sediment leachate values (named zone I). The deeper section of the core with higher Nd/Ca values and no inter-substrate ε_{Nd} offsets is named zone II. Note that depth within sediment core (in metres composite depth) is plotted on a non-linear scale.

4.1.2 Controls on downcore rare earth element distributions

The downcore REE signatures of planktonic foraminifera at Site 980 (shown in Fig. 3bef) are characterized by upper (zone I) and lower (zone II) intervals, with a distinct transition at 2.9 mcd (11.5 ka). Nd/Ca values (Fig. 3b) are consistently relatively low throughout zone I (~700–800 nmol/mol), with higher and more variable values in zone II (900e3000 nmol/mol). Nd/Mn values are also more variable in zone II, with the highest values typically associated with (or close to) H-events. Below the transition at 2.9 mcd, there is less enrichment of heavy REEs over light REEs (Fig. 3e) and cerium anomaly values are closer to 1 (Fig. 3d). A systematic offset between the sediment leachate ε_{Nd} values and the other substrates is also recorded in zone I but is not clearly present in zone II (Fig. 3a). This observation raises the possibility of a link between the processes controlling REE distributions across 2.9 mcd and inter-substrate offsets in ε_{Nd} values. We explore three potential explanations for the distinct difference in behaviour of REEs in the upper (zone I) and lower (zone II) sections of the studied interval. These are (i) exchange between

519 detrital and authigenic phases, (ii) an active redox front in the sediment and (iii) preserved
520 differences between glacial and interglacial bottom water chemistry.

521 The REE signature of bulk sediment can co-vary with lithology (e.g. Sholkovitz,
522 1988). The detrital fraction, however, is typically unreactive, as evidenced by its extraction
523 procedure (Bayon et al., 2002; Jones et al., 1994), and REE concentrations are much lower
524 than in the Fe-Mn oxyhydroxide fraction (Gutjahr et al., 2007). The ε_{Nd} values of bulk
525 sediment at Site 980 (Crocket et al., 2011) are consistently offset towards less radiogenic
526 values than any of the substrates discussed here (Fig. 3a). There is also no clear relation-
527 ship between the relative proportions of radiogenic and unradiogenic IRD and the co-
528 registered foraminiferal ε_{Nd} (see supplementary information). These observations suggest
529 that significant exchange between the detrital and authigenic phases is not the main control
530 on foraminiferal REE distributions.

531 Many of the phases which have been shown to host REEs associated with
532 foraminifera (Fe-Mn (hydr)oxides, organic matter and Mn carbonates) are sensitive to
533 redox conditions (Tachikawa et al., 2014). Therefore, the presence of an active redox front
534 at 2.9 m depth could result in a remobilization and redistribution of foraminiferal REEs.
535 The similarity of shift in REE distribution recorded by both foraminifera and fish debris,
536 however, argues against this explanation at Site 980. The REE signal of fish debris is
537 acquired at shallow depths in the sediment and is relatively resis- tant to diagenesis, with
538 substitution of rare earth elements into the crystal lattice occurring only under more
539 extreme conditions and resulting in a distinctive bell-shaped REE profile (Martin and
540 Scher, 2004; Reynard et al., 1999; Staudigel et al., 1985). This profile is not seen in any of
541 the samples presented here (Fig. 4). In addition, strong negative Ce/Ce* values are

542 preserved in Miocene fish teeth at nearby Site 982 (Martin et al., 2010), similar to that
543 preserved by Holocene (but not glacial) samples at Site 980, suggesting that REE
544 distributions are not reset below the top few metres of sediment. Therefore, it is unlikely
545 that diagenetic redistribution across an active redox front explains the shift in REE
546 distribution in either uncleaned foraminifera or fish debris, supporting our use of fish debris
547 and foraminiferal REE chemistry at Site 980 to reconstruct past oceanographic conditions.
548 The cerium anomaly (Ce/Ce*) is often used to track oxidation because cerium is
549 readily converted from the insoluble Ce (IV) to the soluble Ce (III) phase when water
550 column oxygenation de- creases (Elderfield et al., 1988). It should, however, be noted that
551 Ce/ Ce* preserved by sediment components is not an infallible recorder of local bottom
552 water oxidation, with questions raised regarding the incorporation of REEs into various
553 marine substrates (e.g. German and Elderfield, 1990; Holser, 1997; MacLeod and Irving,
554 1996). In addition, lower Ce/Ce* ratios are recorded in the mod- ern Pacific and Indian
555 Oceans compared to the North Atlantic Ocean; a result which is attributed to a progressive
556 removal of Ce as the age of a bottom water mass increases (German and Elderfield, 1990).
557 The higher Ce/Ce* values at Site 980 during the glacial could therefore indicate a more
558 vigorous overturning circulation than during the Holocene, with several studies supporting
559 vigorous renewal of intermediate waters in the North Atlantic under glacial conditions (e.g.
560 Gherardi et al., 2009; McCave et al., 1995a). An alternative explanation is that the higher
561 Ce/Ce* values in zone II (close to 1; Fig. 3d) in our record indicate that glacial bottom
562 waters at Site 980 had a relatively low oxygen content compared with conditions in the
563 Holocene. A similar increase in both Ce/Ce* and Nd/Ca of uncleaned planktonic
564 foraminifera during the transition into the Holocene has been recorded at Bermuda Rise

565 (Roberts et al., 2012). Glacial-interglacial differences in the degree of oxygenation of
566 shallowly buried sediments have been documented in a number of studies around the world
567 (Jaccard and Galbraith, 2012), with decreased oxygenation of glacial bottom waters re-
568 ported in the intermediate depth northeast Atlantic (Baas et al., 1998; Scho€nfeld et al.,
569 2003). The broad coincidence of the boundary between zone I and II with the climatic
570 transition into the Holocene therefore raises the possibility that the differences in REE
571 behaviour at Site 980 are the product of differences in the degree of pore water oxidation
572 between glacial and interglacial conditions.

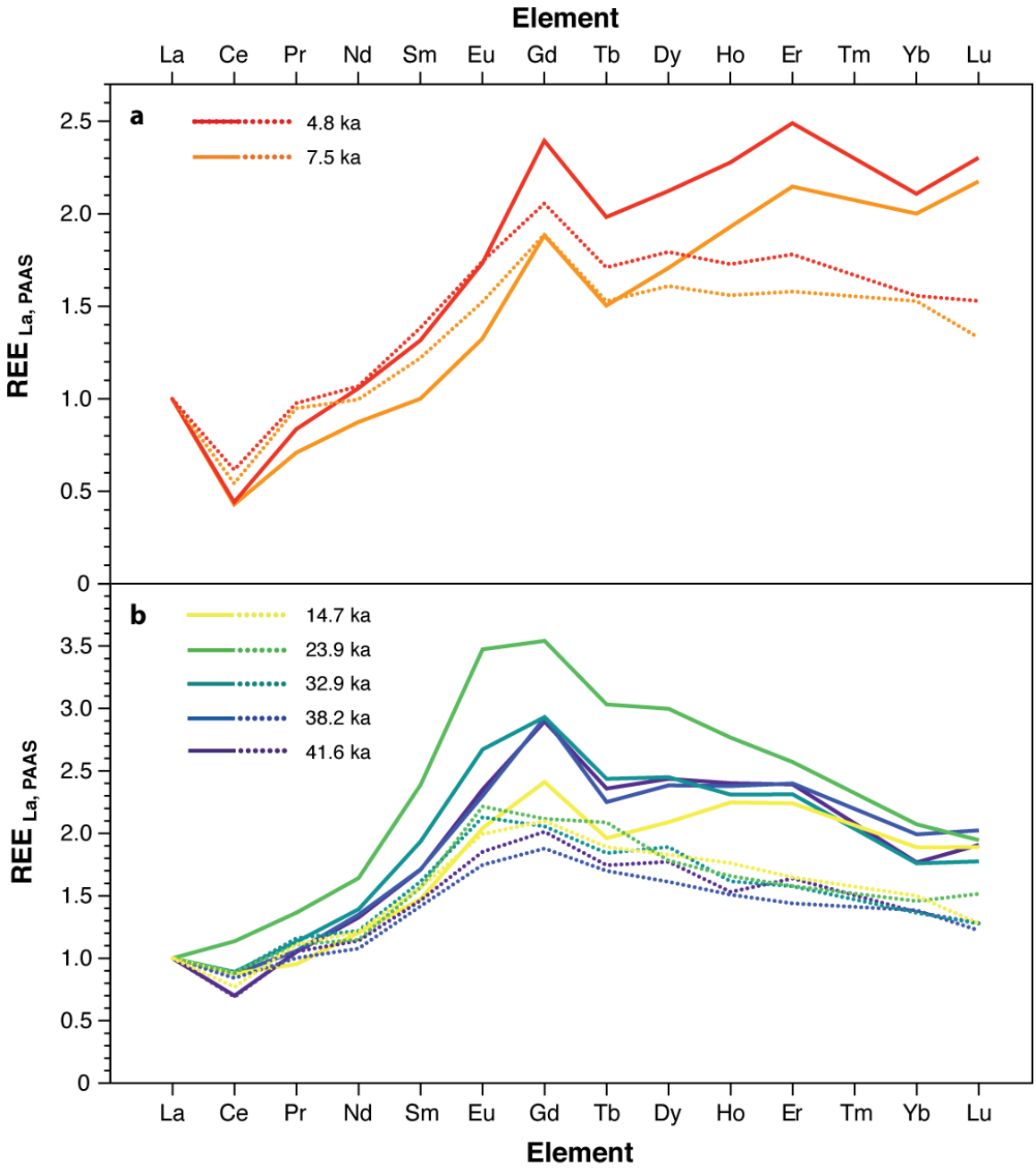

573

574 Fig. 4: Comparison of REE profiles of ODP Site 980 fish debris (dotted lines) and mixed planktonic

575 foraminifera (solid lines). Values are normalised to PAAS and La = 1, with samples from zone I in

576 panel (a) and zone II in panel (b). Sample ages given in figure legend.

577

578 4.1.3 Assessing potential lithogenic influence on ε_{Nd} at Site 980

579 Foraminiferal ε_{Nd} values during the late Holocene (–11.7 ± 0.3) at Site 980 are consistent
580 with the representative signatures of the water masses bathing this site today, however
581 determining whether older ε_{Nd} signatures are also representative of regional water mass
582 chemistry requires further evaluation. The radiogenic signal (-7.9 to -4.2) in foraminiferal
583 ε_{Nd} of the nearby BOFS cores (locations shown in Fig. 1) during the Last Glacial Maximum
584 has been interpreted to reflect labelling of the bottom waters bathing these sites by IRD
585 raining through the water column (Roberts and Piotrowski, 2015). Therefore, before we
586 can use foraminifera-based ε_{Nd} data from Site 980 to determine past variations in water
587 mass sourcing, first we must explore the possibility that exchange with lithogenic material
588 has influenced glacial ε_{Nd} values in our datasets.

589 Three lines of evidence suggest that there was a smaller influence of local
590 modification of water mass chemistry by IRD at ODP Site 980 than the BOFS sites. First,
591 the radiogenic ε_{Nd} values (≥-8) reported by Roberts and Piotrowski (2015) during MIS 2
592 are not recorded at Site 980 (Fig. 5a). Second, we observe ε_{Nd} excursions of opposing signs
593 during H2 and H4, despite lithologically similar IRD assemblages (Fig. 3a and
594 supplementary information). Third, our new IRD records demonstrate that IRD inputs
595 during the last glacial period at Site 980 (typically 0–650 grains/g, peaking at 1450 grains/
596 g during H2) are lower than those recorded at the BOFS sites (400–4700 grains/g (Roberts
597 and Piotrowski, 2015)) (Fig. 5c and d). The same result is also true of the concentrations
598 of volcanic grains, highlighting that the Feni Drift was likely subject to a different IRD
599 depositional regime than the one influencing the BOFS sites during the last glacial period.
600 Although we cannot discount the influence at Site 980 of water masses modified by IRD
601 upstream of our site, and no direct correlation was found between volcanic IRD con-

602 centration and ε_{Nd} values by Roberts and Piotrowski (2015), we suggest that the absence
603 of large volumes of reactive material sinking through the water column at Site 980 during
604 the last glacial period reduced the potential for local modification of water mass chemistry.
605 We therefore suggest that IRD water mass relabelling is not the dominant control on the
606 down core variability in our ε_{Nd} data. Hence, modification of the water column ε_{Nd} by IRD
607 (Roberts and Piotrowski, 2015) may not be significantly problematic in all regions of IRD
608 deposition.

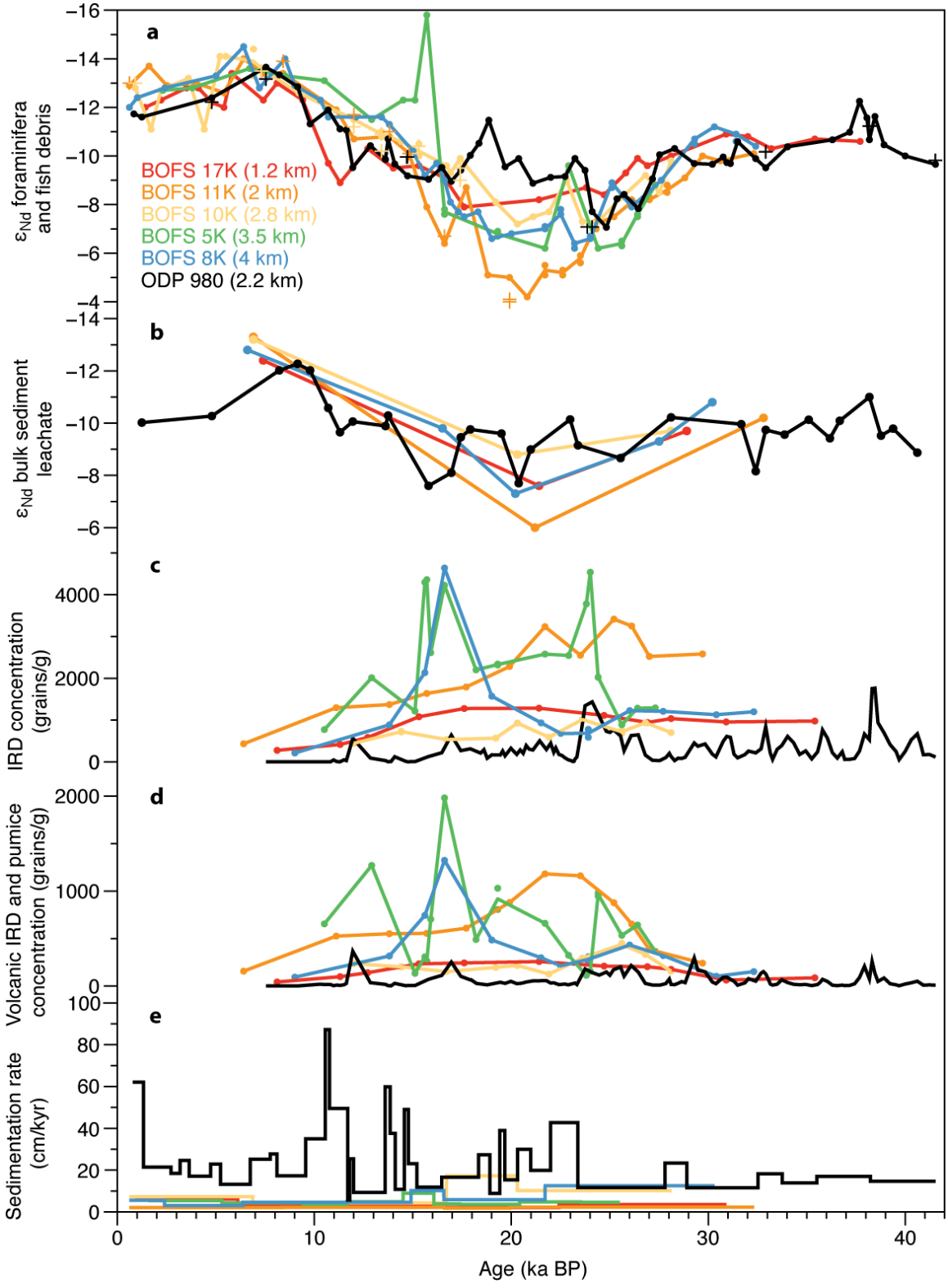

609

610 Fig. 5: Comparison of palaeoclimate records from Site 980 (this study and Crocket et al. (2011))

611 and BOFS sites on and along the southern flank of the Rockall Plateau (Roberts and Piotrowski,

612 2015) (water depths in legend, site locations shown in Fig. 1). (a) Uncleaned foraminifera (solid
613 circles and lines) and fish debris ε_{Nd} (crosses). (b) Bulk sediment leachate ε_{Nd} values. (c)
614 Concentration of IRD grains 150 – 500 μm (Site 980) and >150 μm (BOFS cores (Roberts and
615 Piotrowski, 2015)). (d) Concentration of volcanic IRD (including basalt and mafic and felsic
616 volcanic glasses) and pumice clasts with grain size 150 – 500 μm (Site 980) and >150 μm (BOFS
617 sites, Roberts and Piotrowski (2015)). (e) Sedimentation rates (cm/kyr) based on published age
618 models (BOFS sites, Roberts and Piotrowski (2015)) and this study (Site 980).
619

620 ## 4.2 Water mass changes

621

622 Having established that fish debris and uncleaned planktic foraminifera provide a reliable
623 record of bottom water Nd isotope composition at Site 980, next we combine these ε_{Nd} data
624 with three additional complementary proxies for water mass chemistry (B/Ca, $\delta^{13}C$ and
625 $\delta^{18}O$) to reconstruct oceanographic variability in the mid-depth northeast Atlantic over the
626 past 40,000 years.
627

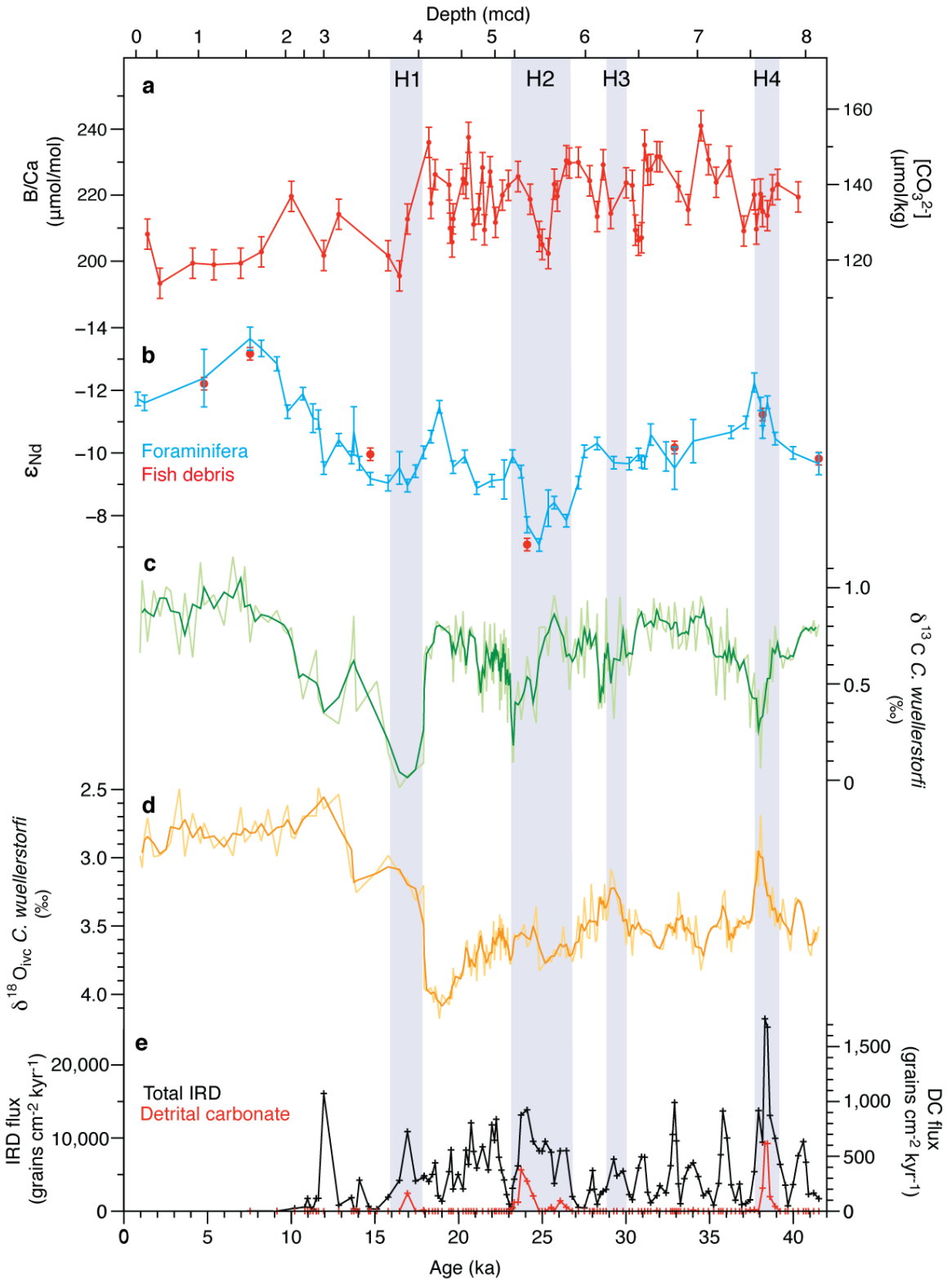

628

629 Fig. 6: Bottom water chemistry shifts at ODP Site 980 during H-events. Shaded bands mark the

630 position of the H-events identified by IRD abundance at Site 980. (a) Bottom water carbonate ion

concentrations reconstructed from B/Ca ratios of benthic foraminifera *C. wuellerstorfi,* with error bars indicating analytical uncertainty (calibration uncertainty ± 10μmol/kg (Yu and Elderfield, 2007)). (b) Neodymium isotope ratios of planktonic foraminifera with ferromanganese coatings not removed (in blue) and fish debris (red) (error bars ±2σ). (c) $\delta^{13}C$ of *C. wuellerstorfi*, with darker line colour marking the three-point running mean. (d) $\delta^{18}O$ of *C. wuellerstorfi*, corrected for global ice volume changes, with darker line colour marking the three-point running mean. (e) Fluxes of ice-rafted debris (black) and detrital carbonate clasts (red) in grains 150 – 500 μm cm^{-2} kyr^{-1}.

4.2.1 Glacial-interglacial variability

In Fig. 6, we present Site 980 fish debris and foraminiferal ε_{Nd} alongside benthic $\delta^{13}C$ and B/Ca ratios for the past 41 ka. A distinct difference in the properties of the water mass bathing Site 980 can be seen between the glacial and Holocene, with glacial waters having a more radiogenic ε_{Nd} signature (Fig. 6b), slightly lighter carbon isotope values (Fig. 6c) and higher [CO_3^{2-}] (indicated by higher benthic foraminiferal B/Ca ratios, Fig. 6a). These obser- vations strongly suggest that the interpretation of Crocket et al. (2011) invoking the persistent dominance of WTROW throughout the last 40 kyr at this site cannot be correct without a significant shift in the properties of WTROW.

Marked similarities exists between the long-term evolution of εNd at Site 980 and deep water sites at the Bermuda Rise (Bo€hm et al., 2015; Gutjahr and Lippold, 2011; Roberts et al., 2010) and South Atlantic Cape Basin (Piotrowski et al., 2005, 2012; Rutberg et al., 2000) (Fig. 7). The Bermuda Rise and Cape Basin records are primarily controlled by mixing between unradiogenic north- ern- and radiogenic southern-sourced waters. An increased contribution of radiogenic southern-sourced waters mixing with northern-sourced waters in the glacial northeast North Atlantic cannot be ruled out on the basis of

Nd isotopes alone, but B/Ca-based reconstructions of carbonate ion concentrations argue against this interpretation. Both modern and glacial SSW typically have low [CO_3^{2-}] (75–95 mmol/mol), whereas modern North Atlantic Deep Water and Nordic Sea overflows are much richer in [CO_3^{2-}] (>100 mmol/mol) (Key et al., 2004; Yu et al., 2008, 2014). Reconstructed glacial carbonate ion concentrations (~130–150 mmol/mol) at Site 980 are higher than those in the Holocene (~115–135 mmol/mol) (Fig. 6), the opposite direction of change as would be expected if an increased glacial presence of southern-sourced waters is the dominant driver of the difference in bottom water chemistry observed at Site 980 between the Holocene and last glacial period.

A reduction in the influence of unradiogenic LSW under glacial conditions (Cottet-Puinel et al., 2004; Hillaire-Marcel et al., 2001) could contribute to the more radiogenic glacial ε_{Nd} signature at Site 980, however, as modern LSW has high [CO_3^{2-}] (Key et al., 2004; Yu et al., 2008), a decrease in glacial LSW influence alone cannot explain the observed bottom water chemistry changes at Site 980, if it is assumed that glacial LSW had similar properties to modern. A decreased export of Mediterranean outflow water (MOW) has been documented under glacial conditions (Zahn et al., 1997), but as modern MOW is moderately radiogenic (-9.4 ± 0.5 (Spivack and Wasserburg, 1988)), a reduction in MOW cannot explain the glacial shift towards more radiogenic bottom waters at Site 980. Alternatively, Rogerson et al. (2005) suggest that the core of MOW deepened which could increase its influence at Site 980, and as MOW has a high modern [CO_3^{2-}], potentially contribute to the observed shift in glacial-interglacial bottom water chemistry. An increased influence of relatively radiogenic and high [CO_3^{2-}] Nordic Sea overflow waters at Site 980 during the last glacial period as suggested by Yu et al. (2008) is an alternative

candidate to explain the more radiogenic and [CO_3^{2-}]-rich glacial bottom water signature at Site 980. It should be noted that an increased influence of overflow waters on bottom water chemistry at Site 980 does not require an increase in overflow current vigour, particularly in light of the decreased contribution of LSW (Cottet-Puinel et al., 2004; Hillaire-Marcel et al., 2001) to the main Atlantic basin during the last glacial period.

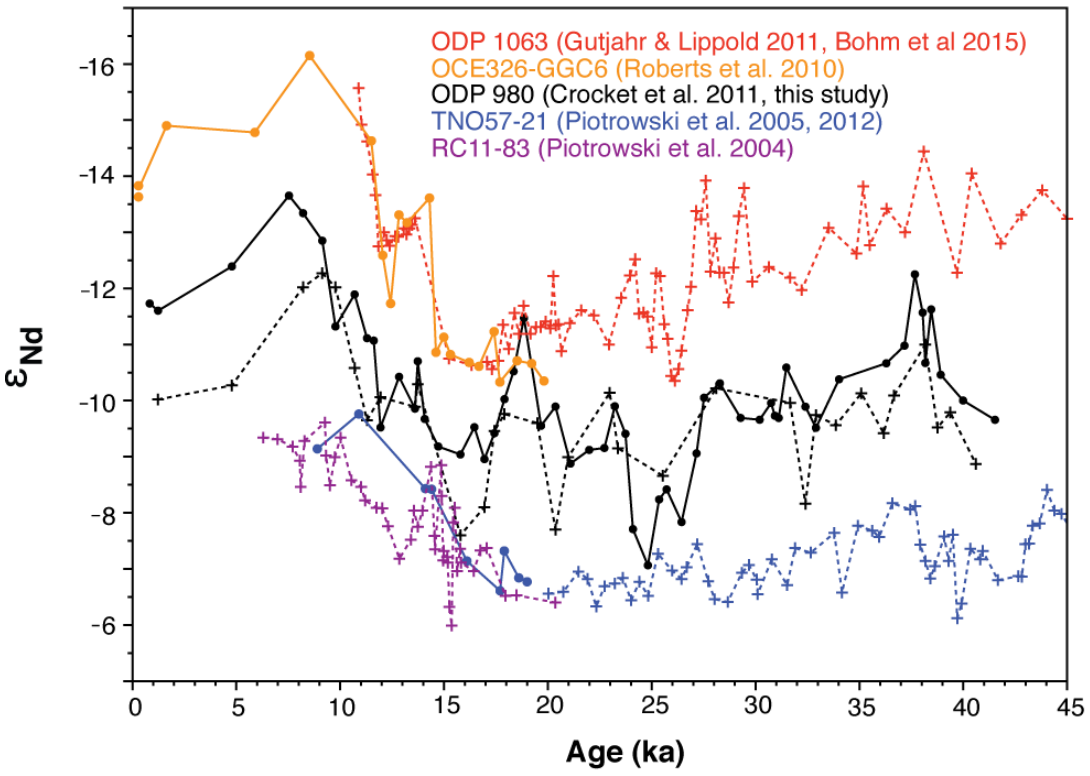

Fig. 7: Comparison of Site 980 uncleaned foraminiferal and bulk sediment leachate ε_{Nd} records (black) with deep sites at the Bermuda Rise (ODP 1063/OCE326-GGC6 in red/orange (Böhm et al., 2015; Gutjahr and Lippold, 2011; Roberts et al., 2010)) and South Atlantic (TNO57-21/RC11-83 in blue/purple Piotrowski, 2012; Piotrowski, 2005; Piotrowski, 2004). Foraminferal ε_{Nd} values are shown with solid lines and filled circles, while bulk sediment leachates are shown with dotted lines and hollow circles. Note that GGC6 bulk sediment leachate values are not shown as these were deemed not to be representative of bottom water chemistry by Roberts et al. (2010).

692

693 4.2.2 Heinrich events

694 Our multi-proxy reconstruction of bottom water properties at Site 980 shows prominent
695 excursions associated with increased concentrations of IRD during each of H-events 4 – 1
696 (Fig. 6). Large shifts in the ε_{Nd} of bottom waters are documented for both H4 (ε_{Nd} = –13.6)
697 and H2 (–7.1), but these excursions are of opposing signs. A small (~ 20 μmol/kg)
698 reduction in bottom water [CO_3^{2-}] is recorded during H2 and just prior to H3, but there is
699 no significant change during H4, and at no point in the record do the values get close to
700 SSW values (75–95 μmol/kg (Key et al., 2004; Yu et al., 2014; Yu et al., 2008)).
701 Excursions towards low benthics $\delta^{13}C$ are recorded during each of the H-events, although
702 typically lagging slightly behind the main IRD peak.

703 Arguably, the most notable feature is the unique expression of each event in our
704 proxy records of bottom water chemistry, with differences in the sign of change, as well as
705 the magnitude of excursions. This simple observation shows that circulation changes in the
706 mid-depth glacial northeast Atlantic are much more complex than simple two component
707 northern- and southern-sourced endmember mixing model. Instead, either three or more
708 water masses must have influenced Site 980 during the last glacial period, or alternatively,
709 shifts in surface ocean properties (particularly in deep water formation regions) or
710 circulation vigour significantly modified the properties of water masses.

711 The surface of the North Atlantic Ocean is thought to have been a highly dynamic
712 environment during the last glacial period, with temporally variable freshwater input from
713 both icebergs and continental sources (Heinrich, 1988; Hemming, 2004; Lekens et al.,
714 2006; Stanford et al., 2011). Fluctuations in sea surface tempera- ture, salinity, sea ice cover

715 and productivity have all been docu- mented in the high northern latitudes (e.g. Dokken et
716 al., 2013; Maslin et al., 1995; van Kreveld, 1996). An increase in sea ice cover has the
717 potential to reduce air-sea exchange in the deep water formation regions, with CO_2 invasion
718 and evasion acting upon both the $d^{13}C$ and carbonate ion concentration of a water mass in
719 a specific ratio (Fig. 8) (Yu et al., 2008). The variability in our data between H-events and
720 non-Heinrich glacial intervals does not follow this trend, therefore we infer that variable
721 sea-ice cover in deep water formation regions is not a major contributor to the variability
722 in bottom water chemistry recorded at Site 980 during H-events. Instead, there is a closer
723 fit to the "biology" slope, which represents the influence of biological regeneration on
724 seawater chemistry and incorporates the effects of organic tissue degrada-tion and $CaCO_3$
725 remineralisation (Yu et al., 2008). The influence of a water mass with increased organic
726 matter remineralisation may therefore explain part of the H-event signals
727 in our proxy records. This signature could reach the site either by increased surface
728 productivity or increased age of the bottom waters reflecting a longer time interval since
729 the water mass was exposed to the atmosphere, either as a result of a rearrangement of
730 circulation patterns, a shift in water mass boundaries or a decrease in circulation vigour.
731 Additional independent proxy records for current vigour such as such as sortable silt
732 (McCave et al., 1995b) or $^{231}Pa/^{230}Th$ (Yu et al., 1996) could therefore prove valuable in
733 better understanding the origin of the observed excursions of bottom water chemistry in
734 the northeast North Atlantic during H-events.
735
736

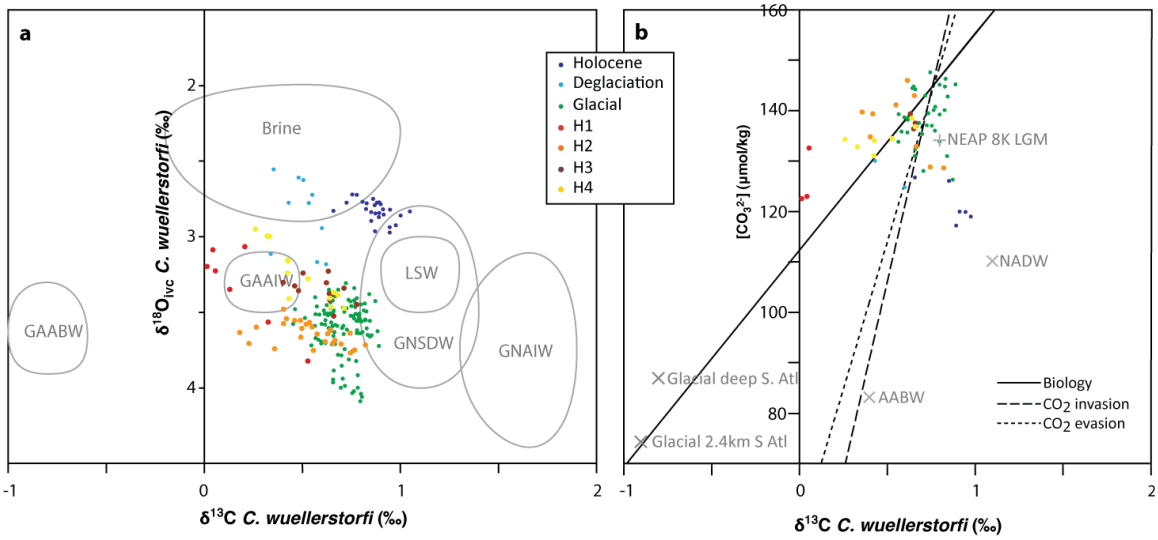

737

738 Fig. 8: Comparison of Site 980 bottom water chemistry to regional water mass signatures. (a) Cross-
739 plot of co-measured oxygen and carbon isotopes of *C. wuellerstorfi* from ODP Site 980. All values
740 are smoothed (3-point running mean), with $\delta^{18}O$ values adjusted for global ice volume changes.
741 Estimated water mass compositions shown in grey, based upon Bertram et al. (1995), Voelker et
742 al. (2006), Meland et al. (2008) and Thornalley et al. (2010). Water masses abbreviations:
743 GAABW: Glacial Antarctic Bottom Water; GAAIW: Glacial Antarctic Intermediate Water; LSW:
744 Labrador Sea Water (Holocene value); GNAIW: Glacial North Atlantic Intermediate Water;
745 GNSDW: Glacial Norwegian Sea Deep Water. Note that the isotopic composition of brines has
746 high uncertainty (e.g. Meland et al., 2008; Thornalley et al., 2010). (b) Cross-plot of $\delta^{13}C$ *C.*
747 *wuellerstorfi* and estimated bottom water $[CO_3^{2-}]$ calculated from *C. wuellerstorfi* B/Ca ratios (see
748 methods). Also shown are lines indicating the calculated slope of co-variance in $\delta^{13}C$ and $[CO_3^{2-}]$
749 generated by biological regeneration and CO_2 invasion/evasion (Yu et al., 2008). Reconstructed
750 water mass signatures are shown in grey (data from Yu et al., 2014; Yu et al., 2008). NEAP 8K is
751 thought to record a strong influence of overflow waters from the Nordic Seas at the Last Glacial
752 Maximum (Yu et al., 2008).

753

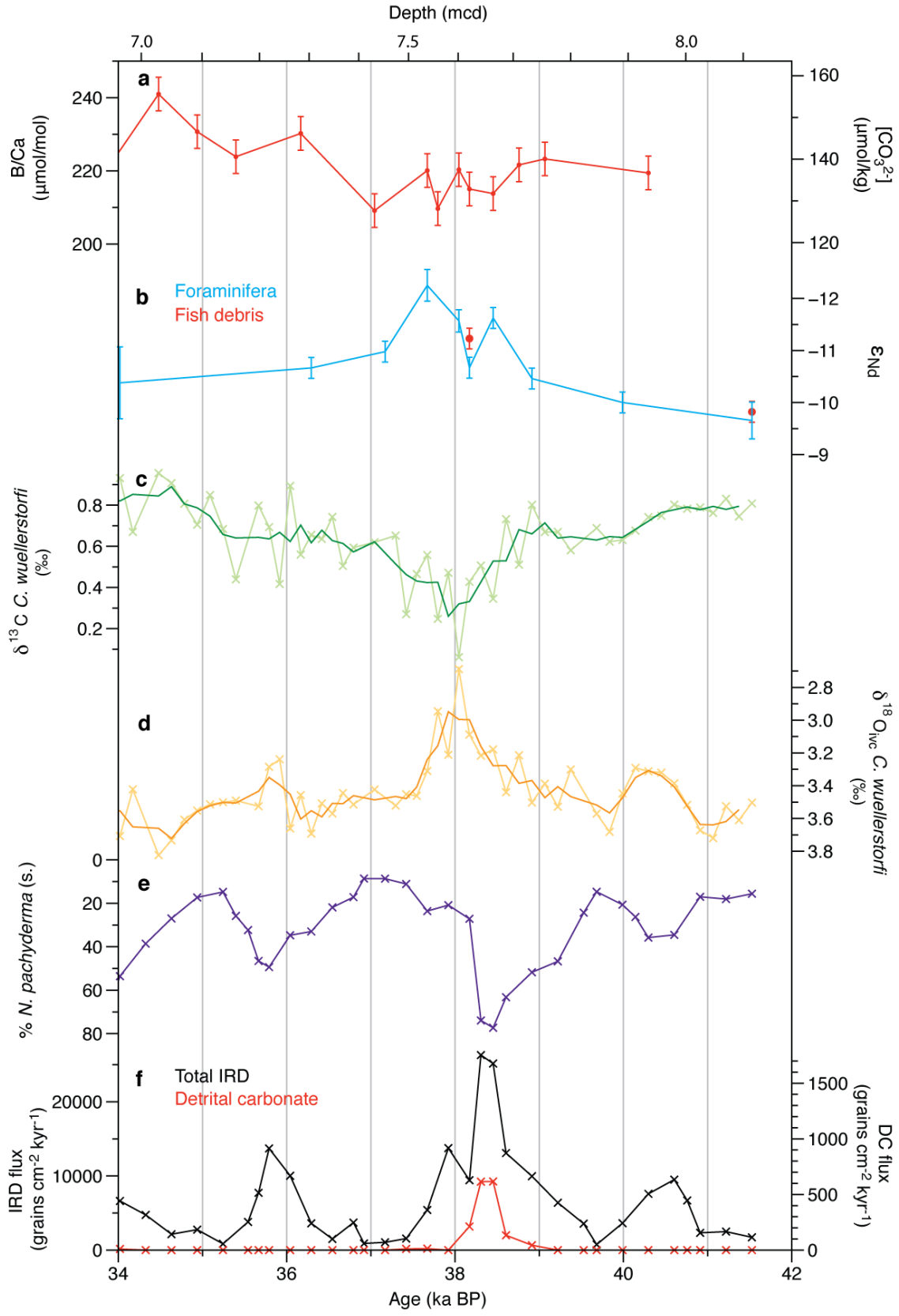
Depth (mcd)
7.0
7.5
8.0
a
B/Ca (µmol/mol)
240
220
200
[CO3 2-] (µmol/kg)
160
140
120
b
Foraminifera
Fish debris
εNd
−12
−11
−10
−9
c
δ13C C. wuellerstorfi (‰)
0.8
0.6
0.4
0.2
d
δ18Oivc C. wuellerstorfi (‰)
2.8
3.0
3.2
3.4
3.6
3.8
e
% N. pachyderma (s.)
0
20
40
60
80
f
Total IRD
Detrital carbonate
IRD flux (grains cm-2 kyr-1)
20000
10000
0
DC flux (grains cm-2 kyr-1)
1500
1000
500
0
34
36
38
40
42
Age (ka BP)

754

Fig. 9: Reconstruction of changes in surface and deep ocean during H4. (a) Bottom water carbonate ion concentrations reconstructed from B/Ca ratios of benthic foraminifera *C. wuellerstorfi* with error bars indicating analytical uncertainty (calibration uncertainty ± 10 μmol/kg (Yu and Elderfield, 2007)). (b) Neodymium isotope ratios of planktonic foraminifera with ferromanganese coatings not removed (in blue) and fish debris (red). Error bars indicate ±2σ. (c) $\delta^{13}C$ of *C. wuellerstorfi*, with darker line colour marking the three-point running mean. (d) $\delta^{18}O$ of *C. wuellerstorfi*, corrected for global ice volume changes, with darker line colour marking the three-point running mean. (e) Percentage of polar species *N. pachyderma* (s.) as a proportion of the total number of planktonic foraminifera. (f) Fluxes of ice-rafted debris (black) and detrital carbonate (red) grains from the 150 – 500 μm size fraction of Site 980 samples.

4.2.2.1 Heinrich event 4

Heinrich event 4 is distinct from the other H-events in our record because it is characterized by an excursion towards unradiogenic ε_{Nd} values and a notable decrease in benthic foraminiferal $\delta^{18}O$ (Figs. 6d and 9). Similar $\delta^{18}O$ excursions have been linked to episodes of brine formation in the Nordic Seas (Dokken and Jansen, 1999; Meland et al., 2008; Vidal et al., 1998), although the origin of the low $d^{18}O$ signature is debated (e.g. Bagniewski et al., 2015; Bauch and Bauch, 2001; Rasmussen and Thomsen, 2009; Stanford et al., 2011). Regardless, a Nordic Sea origin for the waters bathing Site 980 during H4 can likely be dis- counted because modern Nordic Seas Overflows have radiogenic signatures of ε_{Nd} -8.2 ± 0.6 (Lacan and Jeandel, 2004b) while our data record a shift of ~2 ε_{Nd} units towards more unradiogenic values. A very large shift in the neodymium isotope composition of the Nordic Seas (for example, due to overprinting by unradiogenic IRD from Greenland) would be required for the shift in bottom water chemistry recorded at Site 980 to be

779 attributed to increased presence of Nordic Seas Overflows at the site. The main source of
780 unradiogenic waters in the North Atlantic today is the Labrador Sea. LSW generation is
781 thought to have been weaker during the last glacial period, although with some evidence
782 of sinking of brine-rich waters during Heinrich events (Cottet-Puinel et al., 2004; Hillaire-
783 Marcel and de Vernal, 2008; Hillaire-Marcel et al., 2001; Nuttin et al., 2015; Weber et al.,
784 2001).

785 Alternatively, an increase in deep water formation south of the GSR could explain
786 the ε^{Nd} signal at Site 980 during H4 (Duplessy et al., 1980; Labeyrie et al., 1992). Surface
787 waters today in the northeast North Atlantic have ε_{Nd} values of -13 to -14.8 (Lacan and
788 Jeandel, 2004c), although southward migration of the polar front during H-events (e.g.
789 Eynaud et al., 2009) may have resulted in more radiogenic surface water signatures.
790 Reconstructions of surface water properties in the open ocean suggest that they may have
791 been insufficiently dense to sink (Maslin et al., 1995). Alternatively, brine formation, could
792 have occurred on the European and/or Icelandic margins, Rockall Plateau or GSR (Meland
793 et al., 2008; Thornalley et al., 2010), with a possible additional input of waters with low
794 $\delta^{18}O$ and $\delta^{13}C$ signatures from the European continent (e.g. Eynaud et al., 2007; Toucanne
795 et al., 2009).

796

797 4.2.2.2 Heinrich event 2

798 Heinrich event 2 shows a very different signal to H4 in our multi-proxy records.
799 Unlike H4, there is no $\delta^{18}O$ excursion (Fig. 6d), and ε_{Nd} values shift ~2 units towards more
800 radiogenic values (> 8; Fig. 6b). A combination of radiogenic ε_{Nd} and low $\delta^{13}C$ with no
801 concurrent excursion in $\delta^{18}O$ in the Atlantic basin is commonly associated with SSW in

802 the Atlantic (e.g. Jonkers et al., 2015; Piotrowski et al., 2008; Rutberg et al., 2000;
803 Thornalley et al., 2010). We also see a small decrease in carbonate ion concentrations (~20
804 mmol/kg), which supports an increase in the contribution of southern-sourced waters to the
805 northeast North Atlantic. Our reconstructed [CO_3^{2-}] of >120 mmol/kg at Site 980 during
806 H2 is, however, well above modern Antarctic bottom and intermediate waters (~85
807 mmol/kg) (Key et al., 2004; Yu et al., 2008), and even more discrepant with values of ~80
808 mmol/kg reported for deep SSW during the Last Glacial Maximum (Yu et al., 2014), so
809 any southern-sourced water would need to be highly diluted by mixing with northern-
810 sourced endmembers. A alterna- tive source of radiogenic waters with high [CO_3^{2-}] is the
811 Nordic Seas (Lacan and Jeandel, 2004b; Lacan et al., 2012), a possibility consistent with
812 proposed strengthening of GSR overflows into the North Atlantic during H-events (Crocket
813 et al., 2011; Meland et al., 2008; Thornalley et al., 2010).

814 A clear temporal lag (~2 kyr, represented by 30 cm of core) exists between the onset
815 of excursions in ε_{Nd} and $\delta^{13}C$ during H2 (Fig. 10). The initial shift in ε_{Nd} values appears to
816 lead the IRD flux increase slightly (as also observed by Gutjahr and Lippold, (2011)), sug-
817 gesting that major freshwater release linked to IRD deposition across the North Atlantic is
818 not required to initiate the circulation changes associated with H-events, although we
819 cannot rule out the influence of earlier, smaller-scale freshwater releases in other lo-
820 cations. A similar result was obtained by Barker et al. (2015) who find that meltwaters
821 from icebergs do not trigger Northern hemisphere stadial events. Bottom water [CO_3^{2-}]
822 values only start to decrease when stadial conditions are well established. The delayed
823 excursion towards low $\delta^{13}C$ values could be a result of a local or regional pulse in the flux
824 of organic matter to the seafloor (Mackensen et al., 1993), or the flushing of previously

825 poorly ventilated waters once ice-rafting has ceased and circulation vigour is increasing.
826 Alternatively, the observed lag may indicate the presence of multiple phases of AMOC
827 reorganization (Wilson et al., 2014), involving the existence of short-term circulation
828 modes, rather than a simple switch between two distinct AMOC states ('glacial' and 'off')
829 (Rahmstorf, 2002).

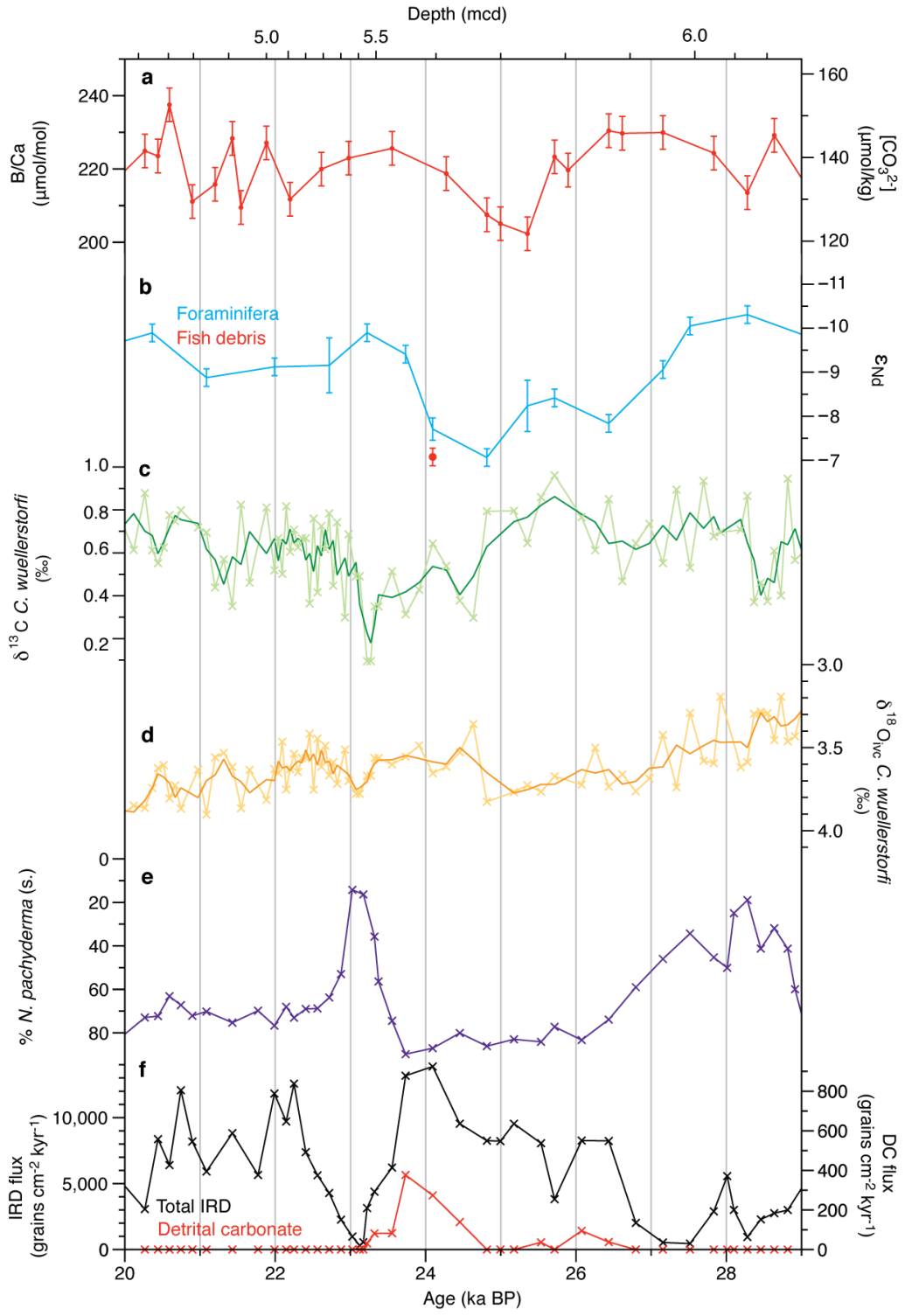

830

831 Fig. 10: Reconstruction of changes in surface and deep ocean during H2. Symbols as Fig. 9.

832

4.2.2.3 Exploration of the differences between H-events

Comparison between multiple H-events allows greater insight into the processes governing AMOC response to fresh water additions. The results of two recent studies (Bo€hm et al., 2015; Lynch-Stieglitz et al., 2014) suggest that an important role in determining the magnitude of oceanographic response to freshwater input is played by the stage in the glacial cycle at which freshwater was released. One of these studies, based on reconstruction of flow through the Florida Straits, suggests that AMOC was least sensitive to fresh- water forcing during full last glacial conditions when stratification of the Atlantic Ocean was at its greatest (Lynch-Stieglitz et al., 2014). The other, a study of water chemistry in the deep North Atlantic on Bermuda Rise, suggests that during the last glacial cycle, the greatest AMOC weakening only occurs when a threshold in continental ice sheet size is crossed, with ice volumes close to their maximum (Bohm et al., 2015).While the magnitude of AMOC perturbation cannot be simply gauged by the amplitude of the excursion in our proxy records, the variability across our data sets strongly suggests a discernible reorganization in ocean structure associated with both H2 (which occurs at close to peak glacial conditions) and H4 (when ice sheets were much smaller (e.g. Siddall et al., 2003)). Our results therefore offer a different perspective, suggesting that the stage of the glacial cycle occupied by H-events may not be the principle factor governing the response of the mid-depth North Atlantic to freshwater release.

The unique chemical signature of intermediate waters during each of the H-events examined (H4 to H1) at Site 980 therefore requires an alternative explanation to changes in global ice volume. Differences in the location, duration and magnitude of melt water inputs have been shown to exert a clear influence over the response of AMOC in modelling

856 experiments (Bigg et al., 2011; Otto-Bliesner and Brady, 2010; Smith and Gregory, 2009).
857 Differences in the IRD assemblages have been documented between H-events (e.g.
858 Grousset et al., 1993; Hall et al., 2011; Peck et al., 2007; Snoeckx et al., 1999), most notably
859 a decreased flux of Hudson Bay- sourced detrital carbonates reaching the North Atlantic
860 during H3 and H6 (e.g. Bond et al., 1992; Hemming, 2004; Hodell and Curtis, 2008),
861 suggesting differences in the relative fresh water contribu- tions from the circum-Atlantic
862 ice sheets. Each H-event is therefore likely associated with different volumes, rates and/or
863 delivery routes of freshwater to the North Atlantic Ocean. These differences are likely to
864 have resulted in shifts in the relative strength of surface water subduction in a number of
865 different potential deep water formation areas. This interpretation of events also offers a
866 potential explanation as to why different events have a different prominence in different
867 locations, and therefore why records from different study regions point to different
868 relationships between global ice volume and AMOC stability (Bohm et al., 2015; Lynch-
869 Stieglitz et al., 2014). AMOC strength has also been shown to exert a strong control over
870 continental hydroclimate (e.g. Burckel et al., 2015; Mulitza et al., 2008), therefore,
871 variations in meltwater inputs between H- events and the resulting AMOC perturbations
872 may have important implications for terrestrial climate.

873 The unique response of intermediate water to fresh water input during each H-event
874 examined (4–1) also raises the possibility of variations in the properties of GNAIW during
875 H-events; a result that may have implications for downstream reconstructions of the
876 strength of exported water from the high northern latitudes at these times. Glacial bottom
877 water chemistry at Site 980 however appears relatively stable between H-events.

878 Our records indicate that a dominance of northern-sourced waters in the mid-depth
879 northeast North Atlantic persisted throughout the last glacial period, but the absence of a
880 strong influence of SSW at our intermediate depth study site does not preclude a dramatic
881 slowdown of the deep ocean during certain H-events (Bohm et al., 2015). In fact, a shoaling
882 of the overturning circulation cell is a feature common to many simulations of fresh- water
883 input to the North Atlantic where AMOC shutdown is incomplete (e.g. Flückiger et al.,
884 2008).
885
886 **5. Summary and Conclusions**
887
888 We investigate the extent to which uncleaned foraminifera, fish debris and bulk sediment
889 leachates can record regionally representative bottom water neodymium isotope
890 compositions in the northeast North Atlantic by examining the isotopic signature of
891 multiple substrates and associated rare earth element distributions. We find that neither
892 local modification of bottom water chemistry by IRD labelling or redistribution of REE at
893 depth within the sediment column exert a strong control over the REE and ε_{Nd} signatures
894 preserved by planktonic foraminifera without their Fe-Mn oxide coatings removed at Site
895 980, making them suitable substrates for palaeoceanographic reconstructions.
896 Foraminiferal and fish debris ε_{Nd} values show good agreement throughout the last 41,000
897 years, however, bulk sediment leachate values are offset towards more radiogenic values
898 by 1–2 ε_{Nd} units throughout the Holocene, which we attribute to the increased influence of
899 fine-grained radiogenic material transported by bottom currents on the sediment leachate

900 values at this time. This result calls for careful evaluation of extracted leachate neodymium
901 isotope compositions for leaching artifacts at North Atlantic drift sites.

902 By combining our new Nd isotope records with three additional proxies for water
903 mass chemistry (B/Ca, $\delta^{13}C$ and $\delta^{18}O$ signatures of *C. wuellerstorfi*), we demonstrate that
904 there is an increased influence of Nordic Seas overflow waters (and not southern-sourced
905 waters) at 2.2 km depth in the Rockall Trough during the late glacial, possibly related in
906 part to a reduction in LSW generation. A dominant presence of SSW at Site 980 at any
907 time within the past 41 kyr is ruled out by reconstructed [CO_3^{2-}] greater than 110 μmol/kg
908 throughout our record. We find that all four H-events within our study interval have
909 different geochemical signatures, with H4 and H2 marked by ε_{Nd} excursions in opposing
910 directions. Unradiogenic ε_{Nd} values and light oxygen and carbon isotope values during H4
911 could indicate an increased contribution of waters from either the Labrador Sea or deep
912 waters forming south of the Greenland-Scotland Ridge, while the radiogenic ε_{Nd} signature
913 recorded during H2 is more likely explained by an increased presence of overflow waters
914 from the Nordic Seas.

915 We find that the stage of the glacial cycle occupied by H-events may not be the
916 principle factor governing the response of the mid- depth North Atlantic to freshwater
917 release. Instead, we suggest that this heterogeneity in the intermediate depth northeast
918 North Atlantic most likely arises due to differences in fresh water input locations,
919 magnitudes and fluxes amongst H-events. The balance of contributions from different
920 source regions to the northern inter- mediate/deep water endmember does not appear to
921 remain constant, with important implications for the chemical signature of GNAIW that
922 is transported downstream during millennial-scale climate events.

Competing financial interests

The authors declare no competing financial interests.

Acknowledgements

This research used samples provided by the Integrated Ocean Drilling (Discovery) Program IODP, which is sponsored by the US National Science Foundation and participating countries under management of Joint Oceanographic Institutions, Inc. We thank Walter Hale and Alex Wülbers for help with sampling, Kirsty Crocket for providing additional samples and Matt Cooper, Andy Milton, Mike Bolshaw and Dave Spanner for analytical support. Heiko Pa€like, David Thornalley and Rachel Mills are thanked for productive discussions and comments on earlier versions of this work. We also thank three anonymous reviewers for their constructive feedback, which greatly improved the manuscript. Funding for this project was provided by NERC studentships to A.J.C. (grant NE/D005728/2) and T.B.C. (NE/I528626/1), with additional funding support from a Royal Society Wolfson Research Merit Award and NERC grants NE/F00141X/1 and NE/I006168/1 to P.A.W. and NE/D00876X/2 to G.L.F.

Appendix A. Supplementary data

Supplementary data related to this article can be found at http://dx.doi.org/10.1016/j.quascirev.2016.08.035.

References

946 Abbott, P.M., Davies, S.M., 2012. Volcanism and the Greenland ice-cores: the tephra
947 record. Earth-Science Reviews 115, 173-191.
948 Adkins, J.F., 2013. The role of deep ocean circulation in setting glacial climates.
949 Paleoceanography 28, 539-561.
950 Alley, R.B., Clark, P.U., Keigwin, L.D., Webb, R.S., 1999. Making sense of millennial-
951 scale climate change. Geophysical Monograph - American Geophysical Union 112, 385-
952 394.
953 Andersen, K.K., Svensson, A., Johnsen, S.J., Rasmussen, S.O., Bigler, M., Röthlisberger,
954 R., Ruth, U., Siggaard-Andersen, M.-L., Steffensen, J.P., Dahl-Jensen, D., Vinther, B.M.,
955 Clausen, H.B., 2006. The Greenland Ice Core Chronology 2005, 15-42 ka. Part 1:
956 constructing the time scale. Quaternary Science Reviews 25, 3246-3257.
957 Arsouze, T., Dutay, J.C., Lacan, F., Jeandel, C., 2009. Reconstructing the Nd oceanic
958 cycle using a coupled dynamical-biogeochemical model. Biogeosciences 6, 2829-2846.
959 Baas, J.H., Schönfeld, J., Zahn, R., 1998. Mid-depth oxygen drawdown during Heinrich
960 events: evidence from benthic foraminiferal community structure, trace-fossil tiering, and
961 benthic □13C at the Portuguese Margin. Marine Geology 152, 25-55.
962 Bagniewski, W., Meissner, K.J., Menviel, L., Brennan, C.E.C.P.A., 2015. Quantification
963 of factors impacting seawater and calcite δ18O during Heinrich Stadials 1 and 4.
964 Paleoceanography 30, 895-911.
965 Ballini, M., Kissel, C., Colin, C., Richter, T., 2006. Deep-water mass source and dynamic
966 associated with rapid climatic variations during the last glacial stage in the North
967 Atlantic: A multiproxy investigation of the detrital fraction of deep-sea sediments.
968 Geochem. Geophys. Geosyst. 7, Q02N01.

969 Bard, E., 1988. Correction of Accelerator Mass Spectrometry ^{14}C Ages Measured in
970 Planktonic Foraminifera: Paleoceanographic Implications. Paleoceanography 3, 635-645.
971 Bard, E., Arnold, M., Mangerud, J., Paterne, M., Labeyrie, L., Duprat, J., Mélières, M.-
972 A., Sønstegaard, E., Duplessy, J.-C., 1994. The North Atlantic atmosphere-sea surface
973 14C gradient during the Younger Dryas climatic event. Earth and Planetary Science
974 Letters 126, 275-287.
975 Barker, S., Chen, J., Gong, X., Jonkers, L., Knorr, G., Thornalley, D., 2015. Icebergs not
976 the trigger for North Atlantic cold events. Nature 520, 333-336.
977 Barker, S., Greaves, M., Elderfield, H., 2003. A study of cleaning procedures used for
978 foraminiferal Mg/Ca paleothermometry. Geochemistry, Geophysics, Geosystems 4, 8407.
979 Bauch, D., Bauch, H.A., 2001. Last glacial benthic foraminiferal δ18O anomalies in the
980 polar North Atlantic: A modern analogue evaluation. Journal of Geophysical Research:
981 Oceans 106, 9135-9143.
982 Bayon, G., German, C.R., Boella, R.M., Milton, J.A., Taylor, R.N., Nesbitt, R.W., 2002.
983 An improved method for extracting marine sediment fractions and its application to Sr
984 and Nd isotopic analysis. Chemical Geology 187, 179-199.
985 Benway, H.M., McManus, J.F., Oppo, D.W., Cullen, J.L., 2010. Hydrographic changes in
986 the eastern subpolar North Atlantic during the last deglaciation. Quaternary Science
987 Reviews 29, 3336-3345.
988 Bertram, C.J., Elderfield, H., Shackleton, N.J., MacDonald, J.A., 1995.
989 Cadmium/Calcium and Carbon Isotope Reconstructions of the Glacial Northeast Atlantic
990 Ocean. Paleoceanography 10, 563-578.

991 Bigg, G.R., Levine, R.C., Green, C.L., 2011. Modelling abrupt glacial North Atlantic
992 freshening: Rates of change and their implications for Heinrich events. Global and
993 Planetary Change 79, 176-192.
994 Blaser, P., Lippold, J., Gutjahr, M., Frank, N., Link, J.M., Frank, M., 2016. Extracting
995 foraminiferal Nd isotope signatures from bulk deep sea sediment by chemical leaching.
996 Chemical Geology.
997 Böhm, E., Lippold, J., Gutjahr, M., Frank, M., Blaser, P., Antz, B., Fohlmeister, J., Frank,
998 N., Andersen, M.B., Deininger, M., 2015. Strong and deep Atlantic meridional
999 overturning circulation during the last glacial cycle. Nature 517, 73-76.
1000 Bond, G., Heinrich, H., Broecker, W., Labeyrie, L., McManus, J., Andrews, J., Huon, S.,
1001 Jantschik, R., Clasen, S., Simet, C., 1992. Evidence for massive discharges of icebergs
1002 into the North Atlantic ocean during the last glacial period. Nature 360, 245-249.
1003 Boyle, E.A., Keigwin, L., 1987. North Atlantic thermohaline circulation during the past
1004 20,000 years linked to high-latitude surface temperature. Nature 330, 35-40.
1005 Boyle, E.A., Keigwin, L.D., 1985. Comparison of Atlantic and Pacific paleochemical
1006 records for the last 215,000 years: changes in deep ocean circulation and chemical
1007 inventories. Earth and Planetary Science Letters 76, 135-150.
1008 Bradtmiller, L.I., McManus, J.F., Robinson, L.F., 2014. 231Pa/230Th evidence for a
1009 weakened but persistent Atlantic meridional overturning circulation during Heinrich
1010 Stadial 1. Nat Commun 5.
1011 Broecker, S.W., Peng, T.-H., 1982. Tracers in the Sea. Eldigo Press, Palisades, NY.
1012 Broecker, W.S., Denton, G.H., 1989. The role of ocean-atmosphere reorganizations in
1013 glacial cycles. Geochimica et Cosmochimica Acta 53, 2465-2501.

1014 Clark, C.D., Hughes, A.L.C., Greenwood, S.L., Jordan, C., Sejrup, H.P., 2012. Pattern
1015 and timing of retreat of the last British-Irish Ice Sheet. Quaternary Science Reviews 44,
1016 112-146.
1017 Cohen, A.S., O'Nions, R.K., Siegenthaler, R., Griffin, W.L., 1988. Chronology of the
1018 pressure-temperature history recorded by a granulite terrain. Contributions to Mineralogy
1019 and Petrology 98, 303-311.
1020 Copard, K., Colin, C., Douville, E., Freiwald, A., Gudmundsson, G., De Mol, B., Frank,
1021 N., 2010. Nd isotopes in deep-sea corals in the North-eastern Atlantic. Quaternary
1022 Science Reviews 29, 2499-2508.
1023 Cottet-Puinel, M., Weaver, A.J., Hillaire-Marcel, C., de Vernal, A., Clark, P.U., Eby, M.,
1024 2004. Variation of Labrador Sea Water formation over the Last Glacial cycle in a climate
1025 model of intermediate complexity. Quaternary Science Reviews 23, 449-465.
1026 Crocker, A., 2014. Coupling of the Cryosphere and Ocean During Intervals of Rapid
1027 Climate Change in the Palaeo Record: A Multi-Proxy Study of the Heinrich Events of the
1028 Last Glacial from the Northeast Atlantic Department of Ocean and Earth Science.
1029 University of Southampton, p. 268.
1030 Crocket, K.C., Vance, D., Gutjahr, M., Foster, G.L., Richards, D.A., 2011. Persistent
1031 Nordic deep-water overflow to the glacial North Atlantic. Geology 39, 515-518.
1032 Curry, W.B., Oppo, D.W., 2005. Glacial water mass geometry and the distribution of
1033 δ13C of ΣCO2 in the western Atlantic Ocean. Paleoceanography 20, PA1017.
1034 Darling, K.F., Kucera, M., Kroon, D., Wade, C.M., 2006. A resolution for the coiling
1035 direction paradox in Neogloboquadrina pachyderma. Paleoceanography 21, PA2011.

1036 Davies, S.M., Abbott, P.M., Pearce, N.J.G., Wastegård, S., Blockley, S.P.E., 2012.
1037 Integrating the INTIMATE records using tephrochronology: rising to the challenge.
1038 Quaternary Science Reviews 36, 11-27.
1039 de Baar, H.J.W., Bacon, M.P., Brewer, P.G., Bruland, K.W., 1985. Rare earth elements in
1040 the Pacific and Atlantic Oceans. Geochimica et Cosmochimica Acta 49, 1943-1959.
1041 de Baar, H.J.W., German, C.R., Elderfield, H., van Gaans, P., 1988. Rare earth element
1042 distributions in anoxic waters of the Cariaco Trench. Geochimica et Cosmochimica Acta
1043 52, 1203-1219.
1044 de Vernal, A., Eynaud, F., Henry, M., Hillaire-Marcel, C., Londeix, L., Mangin, S.,
1045 Matthiessen, J., Marret, F., Radi, T., Rochon, A., Solignac, S., Turon, J.L., 2005.
1046 Reconstruction of sea-surface conditions at middle to high latitudes of the Northern
1047 Hemisphere during the Last Glacial Maximum (LGM) based on dinoflagellate cyst
1048 assemblages. Quaternary Science Reviews 24, 897-924.
1049 Dokken, T.M., Jansen, E., 1999. Rapid changes in the mechanism of ocean convection
1050 during the last glacial period. Nature 401, 458-461.
1051 Dokken, T.M., Nisancioglu, K.H., Li, C., Battisti, D.S., Kissel, C., 2013. Dansgaard-
1052 Oeschger cycles: Interactions between ocean and sea ice intrinsic to the Nordic seas.
1053 Paleoceanography 28, 491-502.
1054 Duplessy, J.-C., Moyes, J., Pujol, C., 1980. Deep water formation in the North Atlantic
1055 Ocean during the last ice age. Nature 286, 479-482.
1056 Dyke, A.S., Andrews, J.T., Clark, P.U., England, J.H., Miller, G.H., Shaw, J., Veillette,
1057 J.J., 2002. The Laurentide and Innuitian ice sheets during the Last Glacial Maximum.
1058 Quaternary Science Reviews 21, 9-31.

1059 Elderfield, H., Greaves, M.J., 1982. The rare earth elements in seawater. Nature 296,
1060 214-219.
1061 Elderfield, H., Whitfield, M., Burton, J.D., Bacon, M.P., Liss, P.S., 1988. The Oceanic
1062 Chemistry of the Rare-Earth Elements. Philosophical Transactions of the Royal Society
1063 of London. Series A, Mathematical and Physical Sciences 325, 105-126.
1064 Ellett, D.J., Martin, J.H.A., 1973. The physical and chemical oceanography of the
1065 Rockall channel. Deep Sea Research and Oceanographic Abstracts 20, 585-625.
1066 Elmore, A.C., Piotrowski, A.M., Wright, J.D., Scrivner, A.E., 2011. Testing the
1067 extraction of past seawater Nd isotopic composition from North Atlantic deep sea
1068 sediments and foraminifera. Geochem. Geophys. Geosyst. 12, Q09008.
1069 Eynaud, F., de Abreu, L.c., Voelker, A., Schˆnfeld, J., Salgueiro, E., Turon, J.-L., Penaud,
1070 A., Toucanne, S., Naughton, F., S·nchez GoÒi, M.F., MalaizÈ, B., Cacho, I., 2009.
1071 Position of the Polar Front along the western Iberian margin during key cold episodes of
1072 the last 45 ka. Geochem. Geophys. Geosyst. 10, Q07U05.
1073 Eynaud, F., Zaragosi, S., Scourse, J.D., Mojtahid, M., Bourillet, J.F., Hall, I.R., Penaud,
1074 A., Locascio, M., Reijonen, A., 2007. Deglacial laminated facies on the NW European
1075 continental margin: The hydrographic significance of British-Irish Ice Sheet deglaciation
1076 and Fleuve Manche paleoriver discharges. Geochem. Geophys. Geosyst. 8, Q06019.
1077 Flückiger, J., Knutti, R., White, J.C., Renssen, H., 2008. Modeled seasonality of glacial
1078 abrupt climate events. Climate Dynamics 31, 633-645.
1079 Funder, S., Hansen, L., 1996. The Greenland ice sheet - a model for its culmination and
1080 decay during and after the last glacial maximum. Bulletin of the Geological Society of
1081 Denmark 42, 137-152.

1082 Garrison, T., 2011. Essentials of oceanography. Thomson Brooks/Cole, Cengage Learing,
1083 Inc.
1084 German, C.R., Elderfield, H., 1990. Application of the Ce anomaly as a paleoredox
1085 indicator: The ground rules. Paleoceanography 5, 823-833.
1086 Gherardi, J.-M., Labeyrie, L., Nave, S., Francois, R., McManus, J.F., Cortijo, E., 2009.
1087 Glacial-interglacial circulation changes inferred from 231Pa/230Th sedimentary record in
1088 the North Atlantic region. Paleoceanography 24, PA2204.
1089 Gierz, P., Lohmann, G., Wei, W., 2015. Response of Atlantic overturning to future
1090 warming in a coupled atmosphere-ocean-ice sheet model. Geophys. Res. Lett. 42, 6811–
1091 6818.
1092 Goldberg, E.D., Koide, M., Schmitt, R.A., Smith, R.H., 1963. Rare-Earth distributions in
1093 the marine environment. Journal of Geophysical Research 68, 4209-4217.
1094 Goldstein, S.L., O'Nions, R.K., Hamilton, P.J., 1984. A Sm-Nd isotopic study of
1095 atmospheric dusts and particulates from major river systems. Earth and Planetary Science
1096 Letters 70, 221-236.
1097 Grandjean, P., Cappetta, H., Michard, A., Albarède, F., 1987. The assessment of REE
1098 patterns and 143Nd/144Nd ratios in fish remains. Earth and Planetary Science Letters 84,
1099 181-196.
1100 Grant, K.M., Rohling, E.J., Bar-Matthews, M., Ayalon, A., Medina-Elizalde, M.,
1101 Ramsey, C.B., Satow, C., Roberts, A.P., 2012. Rapid coupling between ice volume and
1102 polar temperature over the past 150,000 years. Nature 491, 744-747.

1103 Grousset, F.E., Biscaye, P.E., Revel, M., Petit, J.-R., Pye, K., Joussaume, S., Jouzel, J.,
1104 1992. Antarctic (Dome C) ice-core dust at 18 k.y. B.P.: Isotopic constraints on origins.
1105 Earth and Planetary Science Letters 111, 175-182.
1106 Grousset, F.E., Labeyrie, L., Sinko, J.A., Cremer, M., Bond, G., Duprat, J., Cortijo, E.,
1107 Huon, S., 1993. Patterns of Ice-Rafted Detritus in the Glacial North Atlantic (40-55°N).
1108 Paleoceanography 8, 175-192.
1109 Gutjahr, M., Frank, M., Stirling, C.H., Klemm, V., van de Flierdt, T., Halliday, A.N.,
1110 2007. Reliable extraction of a deepwater trace metal isotope signal from Fe-Mn
1111 oxyhydroxide coatings of marine sediments. Chemical Geology 242, 351-370.
1112 Gutjahr, M., Lippold, J., 2011. Early arrival of Southern Source Water in the deep North
1113 Atlantic prior to Heinrich event 2. Paleoceanography 26, PA2101.
1114 Hall, I.R., Colmenero-Hidalgo, E., Zahn, R., Peck, V.L., Hemming, S.R., 2011.
1115 Centennial- to millennial-scale ice-ocean interactions in the subpolar northeast Atlantic
1116 18-41 kyr ago. Paleoceanography 26, PA2224.
1117 Hansen, B., Østerhus, S., 2000. North Atlantic-Nordic Seas exchanges. Progress In
1118 Oceanography 45, 109-208.
1119 Heinrich, H., 1988. Origin and consequences of cyclic ice rafting in the Northeast
1120 Atlantic Ocean during the past 130,000 years. Quaternary Research 29, 142-152.
1121 Hemming, S.R., 2004. Heinrich events: Massive late Pleistocene detritus layers of the
1122 North Atlantic and their global climate imprint. Rev. Geophys. 42, RG1005.
1123 Hillaire-Marcel, C., de Vernal, A., 2008. Stable isotope clue to episodic sea ice formation
1124 in the glacial North Atlantic. Earth and Planetary Science Letters 268, 143-150.

1125 Hillaire-Marcel, C., de Vernal, A., Candon, L., Bilodeau, G., Stoner, J., 2001. Changes of
1126 potential density gradients in the northwestern North Atlantic during the last climatic
1127 cycle based on a multiproxy approach, The Oceans and Rapid Climate Change: Past,
1128 Present, and Future. AGU, Washington, DC, pp. 83-100.
1129 Hodell, D.A., Curtis, J.H., 2008. Oxygen and carbon isotopes of detrital carbonate in
1130 North Atlantic Heinrich Events. Marine Geology 256, 30-35.
1131 Holser, W.T., 1997. Evaluation of the application of rare-earth elements to
1132 paleoceanography. Palaeogeography, Palaeoclimatology, Palaeoecology 132, 309-323.
1133 Innocent, C., Fagel, N., Stevenson, R.K., Hillaire-Marcel, C., 1997. Sm–Nd signature of
1134 modern and late Quaternary sediments from the northwest North Atlantic: Implications
1135 for deep current changes since the Last Glacial Maximum. Earth and Planetary Science
1136 Letters 146, 607-625.
1137 Jaccard, S.L., Galbraith, E.D., 2012. Large climate-driven changes of oceanic oxygen
1138 concentrations during the last deglaciation. Nature Geosci 5, 151-156.
1139 Jacobsen, S.B., Wasserburg, G.J., 1980. Sm-Nd isotopic evolution of chondrites. Earth
1140 and Planetary Science Letters 50, 139-155.
1141 Jansen, E., Fronval, T., Rack, F., Channell, J.E.T., 2000. Pliocene-Pleistocene Ice Rafting
1142 History and Cyclicity in the Nordic Seas During the Last 3.5 Myr. Paleoceanography 15,
1143 709-721.
1144 Jeandel, C., Arsouze, T., Lacan, F., Téchiné, P., Dutay, J.C., 2007. Isotopic Nd
1145 compositions and concentrations of the lithogenic inputs into the ocean: A compilation,
1146 with an emphasis on the margins. Chemical Geology 239, 156-164.

1147 Johnson, C., Sherwin, T., Smythe-Wright, D., Shimmield, T., Turrell, W., 2010. Wyville
1148 Thomson Ridge Overflow Water: Spatial and temporal distribution in the Rockall
1149 Trough. Deep Sea Research Part I: Oceanographic Research Papers 57, 1153-1162.
1150 Jones, C.E., Halliday, A.N., Rea, D.K., Owen, R.M., 1994. Neodymium isotopic
1151 variations in North Pacific modern silicate sediment and the insignificance of detrital
1152 REE contributions to seawater. Earth and Planetary Science Letters 127, 55-66.
1153 Jonkers, L., Zahn, R., Thomas, A., Henderson, G., Abouchami, W., François, R.,
1154 Masque, P., Hall, I.R., Bickert, T., 2015. Deep circulation changes in the central South
1155 Atlantic during the past 145 kyrs reflected in a combined 231Pa/230Th, Neodymium
1156 isotope and benthic record. Earth and Planetary Science Letters 419, 14-21.
1157 Keigwin, L.D., Jones, G.A., Lehman, S.J., Boyle, E.A., 1991. Deglacial meltwater
1158 discharge, North Atlantic Deep Circulation, and abrupt climate change. Journal of
1159 Geophysical Research: Oceans 96, 16811-16826.
1160 Key, R.M., Kozyr, A., Sabine, C.L., Lee, K., Wanninkhof, R., Bullister, J.L., Feely, R.A.,
1161 Millero, F.J., Mordy, C., Peng, T.H., 2004. A global ocean carbon climatology: Results
1162 from Global Data Analysis Project (GLODAP). Global Biogeochemical Cycles 18,
1163 GB4031.
1164 Kissel, C., 2005. Magnetic signature of rapid climatic variations in glacial North Atlantic,
1165 a review. Comptes Rendus Geoscience 337, 908-918.
1166 Kissel, C., Laj, C., Labeyrie, L., Dokken, T., Voelker, A., Blamart, D., 1999. Rapid
1167 climatic variations during marine isotopic stage 3: magnetic analysis of sediments from
1168 Nordic Seas and North Atlantic. Earth and Planetary Science Letters 171, 489-502.

1169 Labeyrie, L.D., Duplessy, J.-C., Duprat, J., Juillet-Leclerc, A., Moyes, J., Michel, E.,
1170 Kallel, N., Shackleton, N.J., 1992. Changes in the vertical structure of the North Atlantic
1171 Ocean between glacial and modern times. Quaternary Science Reviews 11, 401-413.
1172 Lacan, F., Jeandel, C., 2004a. Denmark Strait water circulation traced by heterogeneity in
1173 neodymium isotopic compositions. Deep Sea Research Part I: Oceanographic Research
1174 Papers 51, 71-82.
1175 Lacan, F., Jeandel, C., 2004b. Neodymium isotopic composition and rare earth element
1176 concentrations in the deep and intermediate Nordic Seas: Constraints on the Iceland
1177 Scotland Overflow Water signature. Geochem. Geophys. Geosyst. 5, Q11006.
1178 Lacan, F., Jeandel, C., 2004c. Subpolar Mode Water formation traced by neodymium
1179 isotopic composition. Geophys. Res. Lett. 31, L14306.
1180 Lacan, F., Jeandel, C., 2005. Acquisition of the neodymium isotopic composition of the
1181 North Atlantic Deep Water. Geochem. Geophys. Geosyst. 6, Q12008.
1182 Lacan, F., Tachikawa, K., Jeandel, C., 2012. Neodymium isotopic composition of the
1183 oceans: a compilation of seawater data. Chemical Geology 300-301, 177-184.
1184 Lambelet, M., van de Flierdt, T., Crocket, K., Rehk√§mper, M., Kreissig, K., Coles, B.,
1185 Rijkenberg, M.J.A., Gerringa, L.J.A., de Baar, H.J.W., Steinfeldt, R., 2016. Neodymium
1186 isotopic composition and concentration in the western North Atlantic Ocean: results from
1187 the GEOTRACES GA02 section. Geochimica et Cosmochimica Acta.
1188 Lang, D.C., Bailey, I., Wilson, P.A., Chalk, T.B., Foster, G.L., Gutjahr, M., 2016. In-
1189 cursions of southern-sourced water into the deep North Atlantic during late Pliocene
1190 glacial intensification. Nat. Geosci. 9, 375–379.

1191 Lekens, W.A.H., Sejrup, H.P., Haflidason, H., Knies, J., Richter, T., 2006. Meltwater and
1192 ice rafting in the southern Norwegian Sea between 20 and 40 calendar kyr B.P.:
1193 Implications for Fennoscandian Heinrich events. Paleoceanography 21, PA3013.
1194 Lippold, J., Grützner, J., Winter, D., Lahaye, Y., Mangini, A., Christl, M., 2009. Does
1195 sedimentary 231Pa/230Th from the Bermuda Rise monitor past Atlantic Meridional
1196 Overturning Circulation? Geophysical Research Letters 36, L12601.
1197 Lippold, J., Gutjahr, M., Blaser, P., Christner, E., de Carvalho Ferreira, M.L., Mulitza, S.,
1198 Christl, M., Wombacher, F., Bohm, E., Antz, B., Cartapanis, O., Vogel, H.,
1199 Jaccard, S.L., 2016. Deep water provenance and dynamics of the (de)glacial
1200 Atlantic meridional overturning circulation. Earth Planet. Sci. Lett. 445, 68–78.
1201 Lowe, J.J., Rasmussen, S.O., Björck, S., Hoek, W.Z., Steffensen, J.P., Walker, M.J.C.,
1202 Yu, Z.C., 2008. Synchronisation of palaeoenvironmental events in the North Atlantic
1203 region during the Last Termination: a revised protocol recommended by the INTIMATE
1204 group. Quaternary Science Reviews 27, 6-17.
1205 Lynch-Stieglitz, J., Schmidt, M.W., Gene Henry, L., Curry, W.B., Skinner, L.C., Mulitza,
1206 S., Zhang, R., Chang, P., 2014. Muted change in Atlantic overturning circulation over
1207 some glacial-aged Heinrich events. Nature Geosci 7, 144-150.
1208 Mackensen, A., Hubberten, H.W., Bickert, T., Fischer, G., Fütterer, D.K., 1993. The
1209 δ13C in benthic foraminiferal tests of Fontbotia wuellerstorfi (Schwager) Relative to the
1210 δ13C of dissolved inorganic carbon in Southern Ocean Deep Water: Implications for
1211 glacial ocean circulation models. Paleoceanography 8, 587-610.
1212 MacLeod, K.G., Irving, A.J., 1996. Correlation of cerium anomalies with indicators of
1213 paleoenvironment. Journal of Sedimentary Research 66, 948-955.

1214 Manighetti, B., McCave, I.N., 1995. Late Glacial and Holocene Palaeocurrents Around
1215 Rockall Bank, NE Atlantic Ocean. Paleoceanography 10, 611-626.
1216 Martin, E.E., Blair, S.W., Kamenov, G.D., Scher, H.D., Bourbon, E., Basak, C., Newkirk,
1217 D.N., 2010. Extraction of Nd isotopes from bulk deep sea sediments for
1218 paleoceanographic studies on Cenozoic time scales. Chemical Geology 269, 414-431.
1219 Martin, E.E., Haley, B.A., 2000. Fossil fish teeth as proxies for seawater Sr and Nd
1220 isotopes. Geochimica et Cosmochimica Acta 64, 835-847.
1221 Martin, E.E., Scher, H.D., 2004. Preservation of seawater Sr and Nd isotopes in fossil
1222 fish teeth: bad news and good news. Earth and Planetary Science Letters 220, 25-39.
1223 Maslin, M.A., Shackleton, N.J., Pflaumann, U., 1995. Surface Water Temperature,
1224 Salinity, and Density Changes in the Northeast Atlantic During the Last 45,000 Years:
1225 Heinrich Events, Deep Water Formation, and Climatic Rebounds. Paleoceanography 10,
1226 527-544.
1227 McCartney, M.S., 1992. Recirculating components to the deep boundary current of the
1228 northern North Atlantic. Progress In Oceanography 29, 283-383.
1229 McCave, I.N., Manighetti, B., Beveridge, N.A.S., 1995a. Circulation in the glacial North
1230 Atlantic inferred from grain-size measurements. Nature 374, 149-152.
1231 McCave, I.N., Manighetti, B., Robinson, S.G., 1995b. Sortable silt and fine sediment
1232 size/composition slicing: Parameters for palaeocurrent speed and palaeoceanography.
1233 Paleoceanography 10, 593-610.
1234 McGrath, T., Nolan, G., McGovern, E., 2012. Chemical characteristics of water masses
1235 in the Rockall Trough. Deep Sea Research Part I: Oceanographic Research Papers.

McIntyre, K.L., Howe, J.A., 2009. Bottom-current variability during the last glacial-deglacial transition, Northern Rockall Trough and Faroe Bank Channel, NE Atlantic. Scottish Journal of Geology 45, 43-57.

McLennan, S.M., 1989. Rare earth elements in sedimentary rocks; influence of provenance and sedimentary processes. Reviews in Mineralogy and Geochemistry 21, 169-200.

McManus, J.F., Francois, R., Gherardi, J.M., Keigwin, L.D., Brown-Leger, S., 2004. Collapse and rapid resumption of Atlantic meridional circulation linked to deglacial climate changes. Nature 428, 834-837.

McManus, J.F., Oppo, D.W., Cullen, J.L., 1999. A 0.5-Million-Year Record of Millennial-Scale Climate Variability in the North Atlantic. Science 283, 971-975.

Mearns, E.W., 1988. A samarium-neodymium isotopic survey of modern river sediments from Northern Britain. Chemical Geology: Isotope Geoscience section 73, 1-13.

Meland, M.Y., Dokken, T.M., Jansen, E., Hevrøy, K., 2008. Water mass properties and exchange between the Nordic seas and the northern North Atlantic during the period 23-6 ka: Benthic oxygen isotopic evidence. Paleoceanography 23, PA1210.

Mulitza, S., Prange, M., Stuut, J.-B., Zabel, M., von Dobeneck, T., Itambi, A.C., Nizou, J., Schulz, M., Wefer, G., 2008. Sahel megadroughts triggered by glacial slowdowns of Atlantic meridional overturning. Paleoceanography 23, PA4206.

New, A.L., Smythe-Wright, D., 2001. Aspects of the circulation in the Rockall Trough. Continental Shelf Research 21, 777-810.

North Greenland Ice Core Project Members, Andersen, K.K., Azuma, N., Barnola, J.-M., Bigler, M., Biscaye, P., Caillon, N., Chappellaz, J., Clausen, H.B., Dahl-Jensen, D.,

1259 Fischer, H., Flückiger, J., Fritzsche, D., Fujii, Y., Goto-Azuma, K., Grønvold, K.,
1260 Gundestrup, N.S., Hansson, M., Huber, C., Hvidberg, C.S., Johnsen, S.J., Jonsell, U.,
1261 Jouzel, J., Kipfstuhl, S., Landais, A., Leuenberger, M., Lorrain, R., Masson-Delmotte, V.,
1262 Miller, H., Motoyama, H., Narita, H., Popp, T., Rasmussen, S.O., Raynaud, D.,
1263 Rothlisberger, R., Ruth, U., Samyn, D., Schwander, J., Shoji, H., Siggard-Andersen, M.-
1264 L., Steffensen, J.P., Stocker, T., Sveinbjörnsdóttir, A.E., Svensson, A., Takata, M., Tison,
1265 J.-L., Thorsteinsson, T., Watanabe, O., Wilhelms, F., White, J.W.C., 2004. High-
1266 resolution record of Northern Hemisphere climate extending into the last interglacial
1267 period. Nature 431, 147-151.
1268 Nuttin, L., Maccali, J., Hillaire-Marcel, C., 2015. U, Th and Pa insights into
1269 sedimentological and paleoceanographic changes off Hudson Strait (Labrador Sea)
1270 during the last ~ 37 ka with special attention to methodological issues. Quaternary
1271 Science Reviews 115, 39-49.
1272 O'Nions, R.K., Carter, S.R., Cohen, R.S., Evensen, N.M., Hamilton, P.J., 1978. Pb, Nd
1273 and Sr isotopes in oceanic ferromanganese deposits and ocean floor basalts. Nature 273,
1274 435-438.
1275 Olsen, A., Ninnemann, U., 2010. Large δ13C Gradients in the Preindustrial North
1276 Atlantic Revealed. Science 330, 658-659.
1277 Oppo, D.W., Lehman, S.J., 1993. Mid-Depth Circulation of the Subpolar North Atlantic
1278 During the Last Glacial Maximum. Science 259, 1148-1152.
1279 Oppo, D.W., McManus, J.F., Cullen, J.L., 2003. Palaeo-oceanography: Deepwater
1280 variability in the Holocene epoch. Nature 422, 277-277.

1281 Oppo, D.W., McManus, J.F., Cullen, J.L., 2006. Evolution and demise of the Last
1282 Interglacial warmth in the subpolar North Atlantic. Quaternary Science Reviews 25,
1283 3268-3277.
1284 Otto-Bliesner, B.L., Brady, E.C., 2010. The sensitivity of the climate response to the
1285 magnitude and location of freshwater forcing: last glacial maximum experiments.
1286 Quaternary Science Reviews 29, 56-73.
1287 Paillard, D., Labeyrie, L., Yiou, P., 1996. Macintosh program performs time-series
1288 analysis. Eos. Trans. AGU 77.
1289 Palmer, M.R., Elderfield, H., 1985. Variations in the Nd isotopic composition of
1290 foraminifera from Atlantic Ocean sediments. Earth and Planetary Science Letters 73,
1291 299-305.
1292 Peck, V.L., Hall, I.R., Zahn, R., Grousset, F., Hemming, S.R., Scourse, J.D., 2007. The
1293 relationship of Heinrich events and their European precursors over the past 60 ka BP: a
1294 multi-proxy ice-rafted debris provenance study in the North East Atlantic. Quaternary
1295 Science Reviews 26, 862-875.
1296 Piepgras, D.J., Wasserburg, G.J., Dasch, E.J., 1979. The isotopic composition of Nd in
1297 different ocean masses. Earth and Planetary Science Letters 45, 223-236.
1298 Pin, C., Zalduegui, J.S., 1997. Sequential separation of light rare-earth elements, thorium
1299 and uranium by miniaturized extraction chromatography: Application to isotopic analyses
1300 of silicate rocks. Analytica Chimica Acta 339, 79-89.
1301 Piotrowski, A.M., Galy, A., Nicholl, J.A.L., Roberts, N., Wilson, D.J., Clegg, J.A., Yu,
1302 J., 2012. Reconstructing deglacial North and South Atlantic deep water sourcing using
1303 foraminiferal Nd isotopes. Earth and Planetary Science Letters 357-358, 289-297.

1304 Piotrowski, A.M., Goldstein, S.L., Hemming, S.R., Fairbanks, R.G., 2005. Temporal
1305 Relationships of Carbon Cycling and Ocean Circulation at Glacial Boundaries. Science
1306 307, 1933-1938.
1307 Piotrowski, A.M., Goldstein, S.L., Hemming, S.R., Fairbanks, R.G., 2004. Intensifica-
1308 tion and variability of ocean thermohaline circulation through the last degla- ciation.
1309 Earth Planet. Sci. Lett. 225, 205–220.
1310 Piotrowski, A.M., Goldstein, S.L., Hemming, S.R., Fairbanks, R.G., Zylberberg, D.R.,
1311 2008. Oscillating glacial northern and southern deep water formation from combined
1312 neodymium and carbon isotopes. Earth and Planetary Science Letters 272, 394–405.
1313 Rae, J.W.B., Foster, G.L., Schmidt, D.N., Elliott, T., 2011. Boron isotopes and B/Ca in
1314 benthic foraminifera: Proxies for the deep ocean carbonate system. Earth and Planetary
1315 Science Letters 302, 403-413.
1316 Rahmstorf, S., 2002. Ocean circulation and climate during the past 120,000 years. Nature
1317 419, 207-214.
1318 Rasmussen, S.O., Andersen, K.K., Svensson, A.M., Steffensen, J.P., Vinther, B.M.,
1319 Clausen, H.B., Siggaard-Andersen, M.L., Johnsen, S.J., Larsen, L.B., Dahl-Jensen, D.,
1320 Bigler, M., Röthlisberger, R., Fischer, H., Goto-Azuma, K., Hansson, M.E., Ruth, U.,
1321 2006. A new Greenland ice core chronology for the last glacial termination. J. Geophys.
1322 Res. 111, D06102.
1323 Rasmussen, T.L., Thomsen, E., 2009. Stable isotope signals from brines in the Barents
1324 Sea: Implications for brine formation during the last glaciation. Geology 37, 903-906.
1325 Reimer, P.J., Bard, E., Bayliss, A., Beck, J.W., Blackwell, P.G., Bronk Ramsey, C.,
1326 Buck, C.E., Cheng, H., Edwards, R.L., Friedrich, M., Grootes, P.M., Guilderson, T.P.,

1327 Haflidason, H., Hajdas, I., Hatté, C., Heaton, T.J., Hoffmann, D.L., Hogg, A.G., Hughen,
1328 K.A., Kaiser, K.F., Kromer, B., Manning, S.W., Niu, M., Reimer, R.W., Richards, D.A.,
1329 Scott, E.M., Southon, J.R., Staff, R.A., Turney, C.S.M., van der Plicht, J., 2013. IntCal13
1330 and Marine13 Radiocarbon Age Calibration Curves 0–50,000 Years cal BP.
1331 Reynard, B., Lécuyer, C., Grandjean, P., 1999. Crystal-chemical controls on rare-earth
1332 element concentrations in fossil biogenic apatites and implications for
1333 paleoenvironmental reconstructions. Chemical Geology 155, 233-241.
1334 Rickli, J., Gutjahr, M., Vance, D., Fischer-Gödde, M., Hillenbrand, C.-D., Kuhn, G.,
1335 2014. Neodymium and hafnium boundary contributions to seawater along the West
1336 Antarctic continental margin. Earth and Planetary Science Letters 394, 99-110.
1337 Roberts, N.L., Piotrowski, A.M., 2015. Radiogenic Nd isotope labeling of the northern
1338 NE Atlantic during MIS 2. Earth and Planetary Science Letters 423, 125-133.
1339 Roberts, N.L., Piotrowski, A.M., Elderfield, H., Eglinton, T.I., Lomas, M.W., 2012. Rare
1340 earth element association with foraminifera. Geochimica et Cosmochimica Acta 94, 57-
1341 71.
1342 Roberts, N.L., Piotrowski, A.M., McManus, J.F., Keigwin, L.D., 2010. Synchronous
1343 Deglacial Overturning and Water Mass Source Changes. Science 327, 75-78.
1344 Robinson, L.F., Adkins, J.F., Keigwin, L.D., Southon, J., Fernandez, D.P., Wang, S.L.,
1345 Scheirer, D.S., 2005. Radiocarbon Variability in the Western North Atlantic During the
1346 Last Deglaciation. Science 310, 1469-1473.
1347 Rogerson, M., Rohling, E.J., Weaver, P.P.E., Murray, J.W.C.P., 2005. Glacial to
1348 interglacial changes in the settling depth of the Mediterranean Outflow plume.
1349 Paleoceanography 20, n/a-n/a.

1350 Ruddiman, W.F., 1977. Late Quaternary deposition of ice-rafted sand in the subpolar
1351 North Atlantic (lat 40° to 65°N). Geological Society of America Bulletin 88, 1813-1827.
1352 Rutberg, R.L., Hemming, S.R., Goldstein, S.L., 2000. Reduced North Atlantic Deep
1353 Water flux to the glacial Southern Ocean inferred from neodymium isotope ratios. Nature
1354 405, 935-938.
1355 Sarbas, B., Nohl, U., 2008. The GEOROC database as part of a growing geoinformatics
1356 network, 2008 Geoinformatics conference.
1357 Sarmiento, J.L., Gruber, N., 2004. Ocean Biogeochemical Dynamics. Princeton
1358 University Press, Princeton, NJ.
1359 Sarnthein, M., Winn, K., Jung, S.J.A., Duplessy, J.-C., Labeyrie, L., Erlenkeuser, H.,
1360 Ganssen, G., 1994. Changes in East Atlantic Deepwater Circulation Over the Last 30,000
1361 years: Eight Time Slice Reconstructions. Paleoceanography 9, 209-267.
1362 Schönfeld, J., Zahn, R., de Abreu, L., 2003. Surface and deep water response to rapid
1363 climate changes at the Western Iberian Margin. Global and Planetary Change 36, 237-
1364 264.
1365 Sejrup, H.P., Hjelstuen, B.O., Torbjørn Dahlgren, K.I., Haflidason, H., Kuijpers, A.,
1366 Nygård, A., Praeg, D., Stoker, M.S., Vorren, T.O., 2005. Pleistocene glacial history of the
1367 NW European continental margin. Marine and Petroleum Geology 22, 1111-1129.
1368 Shackleton, N.J., Opdyke, N.D., 1973. Oxygen isotope and palaeomagnetic stratigraphy
1369 of Equatorial Pacific core V28-238: Oxygen isotope temperatures and ice volumes on a
1370 10^5 year and 10^6 year scale. Quaternary Research 3, 39-55.

1371 Shipboard Scientific Party, 1996. Sites 980/981, in: Jansen, E., Raymo, M.E., Blum P. et
1372 al. (Eds.), Proceedings of the Ocean Drilling Program, Initial Reports. College station,
1373 TX, pp. 49-90.
1374 Sholkovitz, E.R., 1988. Rare earth elements in the sediments of the North Atlantic Ocean,
1375 Amazon Delta, and East China Sea; reinterpretation of terrigenous input patterns to the
1376 oceans. American Journal of Science 288, 236-281.
1377 Siddall, M., Rohling, E.J., Almogi-Labin, A., Hemleben, C., Meischner, D., Schmelzer,
1378 I., Smeed, D.A., 2003. Sea-level fluctuations during the last glacial cycle. Nature 423,
1379 853-858.
1380 Sigman, D.M., Boyle, E.A., 2000. Glacial/interglacial variations in atmospheric carbon
1381 dioxide. Nature 407, 859-869.
1382 Sigman, D.M., Hain, M.P., Haug, G.H., 2010. The polar ocean and glacial cycles in
1383 atmospheric CO2 concentration. Nature 466, 47-55.
1384 Singarayer, J.S., Valdes, P.J., 2010. High-latitude climate sensitivity to ice-sheet forcing
1385 over the last 120 kyr. Quaternary Science Reviews 29, 43-55.
1386 Smith, R.S., Gregory, J.M., 2009. A study of the sensitivity of ocean overturning
1387 circulation and climate to freshwater input in different regions of the North Atlantic.
1388 Geophysical Research Letters 36, L15701.
1389 Snoeckx, H., Grousset, F., Revel, M., Boelaert, A., 1999. European contribution of ice-
1390 rafted sand to Heinrich layers H3 and H4. Marine Geology 158, 197-208.
1391 Spivack, A.J., Wasserburg, G.J., 1988. Neodymium isotopic composition of the
1392 Mediterranean outflow and the eastern North Atlantic. Geochimica et Cosmochimica
1393 Acta 52, 2767-2773.

1394 Stanford, J.D., Rohling, E.J., Bacon, S., Roberts, A.P., Grousset, F.E., Bolshaw, M.,
1395 2011. A new concept for the paleoceanographic evolution of Heinrich event 1 in the
1396 North Atlantic. Quaternary Science Reviews 30, 1047-1066.
1397 Staudigel, H., Doyle, P., Zindler, A., 1985. Sr and Nd isotope systematics in fish teeth.
1398 Earth and Planetary Science Letters 76, 45-56.
1399 Stern, J.V., Lisiecki, L.E., 2013. North Atlantic circulation and reservoir age changes
1400 over the past 41,000 years. Geophysical Research Letters 40, 3693-3697.
1401 Stichel, T., Frank, M., Rickli, J., Haley, B.A., 2012. The hafnium and neodymium isotope
1402 composition of seawater in the Atlantic sector of the Southern Ocean. Earth and Planetary
1403 Science Letters 317,Äì318, 282-294.
1404 Stille, P., 1992. Nd-Sr isotope evidence for dramatic changes of paleocurrents in the
1405 Atlantic Ocean during the past 80 m.y. Geology 20, 387-390.
1406 Stille, P., Fischer, H., 1990. Secular variation in the isotopic composition of Nd in Tethys
1407 seawater. Geochimica et Cosmochimica Acta 54, 3139-3145.
1408 Stuiver, M., Reimer, P.J., 1993. Extended ^{14}C database and revised CALIB radiocarbon
1409 calibration program. Radiocarbon 35, 215-230.
1410 Stuiver, M., Reimer, P.J., Reimer, R.W., 2005. CALIB 5.0.
1411 Svensson, A., Andersen, K.K., Bigler, M., Clausen, H.B., Dahl-Jensen, D., Davies, S.M.,
1412 Johnsen, S.J., Muscheler, R., Parrenin, F., Rasmussen, S.O., Röthlisberger, R., Seierstad,
1413 I., Steffensen, J.P., Vinther, B.M., 2008. A 60 000 year Greenland stratigraphic ice core
1414 chronology. Clim. Past 4, 47-57.

1415 Swingedouw, D., Mignot, J., Braconnot, P., Mosquet, E., Kageyama, M., Alkama, R.,
1416 2009. Impact of Freshwater Release in the North Atlantic under Different Climate
1417 Conditions in an OAGCM. Journal of Climate 22, 6377-6403.
1418 Tachikawa, K., Athias, V., Jeandel, C., 2003. Neodymium budget in the modern ocean
1419 and paleo-oceanographic implications. J. Geophys. Res. 108, 3254.
1420 Tachikawa, K., Jeandel, C., Roy-Barman, M., 1999. A new approach to the Nd residence
1421 time in the ocean: the role of atmospheric inputs. Earth and Planetary Science Letters
1422 170, 433-446.
1423 Tachikawa, K., Piotrowski, A.M., Bayon, G., 2014. Neodymium associated with
1424 foraminiferal carbonate as a recorder of seawater isotopic signatures. Quaternary Science
1425 Reviews 88, 1-13.
1426 Tanaka, T., Togashi, S., Kamioka, H., Amakawa, H., Kagami, H., Hamamoto, T.,
1427 Yuhara, M., Orihashi, Y., Yoneda, S., Shimizu, H., Kunimaru, T., Takahashi, K., Yanagi,
1428 T., Nakano, T., Fujimaki, H., Shinjo, R., Asahara, Y., Tanimizu, M., Dragusanu, C.,
1429 2000. JNdi-1: a neodymium isotopic reference in consistency with LaJolla neodymium.
1430 Chemical Geology 168, 279-281.
1431 Taylor, S.R., McLennan, S.M., 1985. The continental crust: its composition and
1432 evolution. Blackwell, Oxford.
1433 Thornalley, D.J.R., Barker, S., Becker, J., Hall, I.R., Knorr, G., 2013. Abrupt changes in
1434 deep Atlantic circulation during the transition to full glacial conditions.
1435 Paleoceanography 28, 253-262.

1436 Thornalley, D.J.R., Bauch, H.A., Gebbie, G., Guo, W., Ziegler, M., Bernasconi, S.M.,
1437 Barker, S., Skinner, L.C., Yu, J., 2015. A warm and poorly ventilated deep Arctic
1438 Mediterranean during the last glacial period. Science 349, 706-710.
1439 Thornalley, D.J.R., Elderfield, H., McCave, I.N., 2010. Intermediate and deep water
1440 paleoceanography of the northern North Atlantic over the past 21,000 years.
1441 Paleoceanography 25, PA1211.
1442 Toucanne, S., Zaragosi, S., Bourillet, J.F., Cremer, M., Eynaud, F., Van Vliet-Lanoë, B.,
1443 Penaud, A., Fontanier, C., Turon, J.L., Cortijo, E., Gibbard, P.L., 2009. Timing of
1444 massive 'Fleuve Manche' discharges over the last 350 kyr: insights into the European ice-
1445 sheet oscillations and the European drainage network from MIS 10 to 2. Quaternary
1446 Science Reviews 28, 1238-1256.
1447 van de Flierdt, T., Robinson, L.F., Adkins, J.F., Hemming, S.R., Goldstein, S.L., 2006.
1448 Temporal stability of the neodymium isotope signature of the Holocene to glacial North
1449 Atlantic. Paleoceanography 21, PA4102.
1450 van Kreveld, S.A., 1996. Northeast Atlantic Late Quaternary planktic Foraminifera as
1451 primary productivity and water mass indicators. Scripta Geologica 113, 23-91.
1452 Vance, D., Thirlwall, M., 2002. An assessment of mass discrimination in MC-ICPMS
1453 using Nd isotopes. Chemical Geology 185, 227-240.
1454 Vaughan, D.G., Comiso, J.C., Allison, I., Carrasco, J., Kaser, G., Kwok, R., Mote, P.,
1455 Murray, T., Paul, F., Ren, J., Rignot, E., Solomina, O., Steffen, K., Zhang, T., 2013.
1456 Observations: Cryosphere, in: Stocker, T.F., Qin, D., Plattner, G.-K., Tignor, M., Allen,
1457 S.K., Boschung, J., Nauels, A., Xia, Y., Bex, V., Midgley, P.M. (Eds.), Climate Change
1458 2013: The Physical Science Basis. Contribution of Working Group I to the Fifth

1459 Assessment Report of the Intergovernmental Panel on Climate Change. Cambridge
1460 University Press, Cambridge, United Kingdom and New York, NY, USA.
1461 Vidal, L., Labeyrie, L., Cortijo, E., Arnold, M., Duplessy, J.C., Michel, E., Becqué, S.,
1462 van Weering, T.C.E., 1997. Evidence for changes in the North Atlantic Deep Water
1463 linked to meltwater surges during the Heinrich events. Earth and Planetary Science
1464 Letters 146, 13-27.
1465 Vidal, L., Labeyrie, L., van Weering, T.C.E., 1998. Benthic δ18O Records in the North
1466 Atlantic Over the Last Glacial Period (60-10 kyr): Evidence for Brine Formation.
1467 Paleoceanography 13, 245-251.
1468 Vinther, B.M., Clausen, H.B., Johnsen, S.J., Rasmussen, S.O., Andersen, K.K., Buchardt,
1469 S.L., Dahl-Jensen, D., Seierstad, I.K., Siggaard-Andersen, M.L., Steffensen, J.P.,
1470 Svensson, A., Olsen, J., Heinemeier, J., 2006. A synchronized dating of three Greenland
1471 ice cores throughout the Holocene. J. Geophys. Res. 111, D13102.
1472 Voelker, A.H.L., Lebreiro, S.M., Schönfeld, J., Cacho, I., Erlenkeuser, H., Abrantes, F.,
1473 2006. Mediterranean outflow strengthening during northern hemisphere coolings: A salt
1474 source for the glacial Atlantic? Earth and Planetary Science Letters 245, 39-55.
1475 Waelbroeck, C., Duplessy, J.-C., Michel, E., Labeyrie, L., Paillard, D., Duprat, J., 2001.
1476 The timing of the last deglaciation in North Atlantic climate records. Nature 412, 724-
1477 727.
1478 Weber, M.E., Mayer, L.A., Hillaire-Marcel, C., Bilodeau, G., Rack, F., Hiscott, R.N.,
1479 Aksu, A.E., 2001. Derivation of δ18O from Sediment Core Log Data: Implications for
1480 Millennial-Scale Climate Change in the Labrador Sea. Paleoceanography 16, 503-514.

1481 Wei, R., Abouchami, W., Zahn, R., Masque, P., 2015. Deep circulation changes in the
1482 South Atlantic since the Last Glacial Maximum from Nd isotope and multi-proxy
1483 records. Earth and Planetary Science Letters 434, 18-29.
1484 Wilson, D.J., Crocket, K.C., van de Flierdt, T., Robinson, L.F., Adkins, J.F., 2014.
1485 Dynamic intermediate ocean circulation in the North Atlantic during Heinrich Stadial 1:
1486 A radiocarbon and neodymium isotope perspective. Paleoceanography, 2014PA002674.
1487 Wilson, D.J., Piotrowski, A.M., Galy, A., Banakar, V.K.C.P.A., 2015. Interhemispheric
1488 controls on deep ocean circulation and carbon chemistry during the last two glacial
1489 cycles. Paleoceanography 30, 621-641.
1490 Wilson, D.J., Piotrowski, A.M., Galy, A., Clegg, J.A., 2013. Reactivity of neodymium
1491 carriers in deep sea sediments: implications for boundary exchange and
1492 paleoceanography. Geochimica et Cosmochimica Acta 109, 197-221.
1493 Wilson, D.J., Piotrowski, A.M., Galy, A., McCave, I.N., 2012. A boundary exchange
1494 influence on deglacial neodymium isotope records from the deep western Indian Ocean.
1495 Earth and Planetary Science Letters 341–344, 35-47.
1496 Yu, E.-F., Francois, R., Bacon, M.P., 1996. Similar rates of modern and last-glacial ocean
1497 thermohaline circulation inferred from radiochemical data. Nature 379, 689-694.
1498 Yu, J., Anderson, R.F., Jin, Z., Menviel, L., Zhang, F., Ryerson, F.J., Rohling, E.J., 2014.
1499 Deep South Atlantic carbonate chemistry and increased interocean deep water exchange
1500 during last deglaciation. Quaternary Science Reviews 90, 80-89.
1501 Yu, J., Elderfield, H., 2007. Benthic foraminiferal B/Ca ratios reflect deep water
1502 carbonate saturation state. Earth and Planetary Science Letters 258, 73-86.

1503 Yu, J., Elderfield, H., Piotrowski, A.M., 2008. Seawater carbonate ion-δ13C systematics
1504 and application to glacial-interglacial North Atlantic ocean circulation. Earth and
1505 Planetary Science Letters 271, 209-220.
1506 Zahn, R., Schönfeld, J., Kudrass, H.-R., Park, M.-H., Erlenkeuser, H., Grootes, P., 1997.
1507 Thermohaline Instability in the North Atlantic During Meltwater Events: Stable Isotope
1508 and Ice-Rafted Detritus Records from Core SO75-26KL, Portuguese Margin.
1509 Paleoceanography 12, 696-710.
1510
1511